A *Legionella pneumophila* effector impedes host gene silencing to promote virulence

Justine Toinon[1], Monica Rolando[2], Magali Charvin[1], Didier Filopon[1], Lionel Schiavolin[1], Khadeeja Adam Sy[1], Hai-Chi Vu[1], Sarah Gallois-Montbrun[3], Antoine Alam[4], Christophe Rusniok[2], Bérangère Lombard[5], Damarys Loew[5], Carmen Buchrieser[2, *], Lionel Navarro[1, *, #]

[1] Institut de Biologie de l'Ecole Normale Supérieure (IBENS), Centre National de la Recherche Scientifique (CNRS), Institut National de la Santé et de la Recherche Médicale (INSERM), Université de recherche Paris, Sciences & Lettres (PSL), 75005 Paris, France.

[2] Institut Pasteur, Université de Paris, Biologie des Bactéries Intracellulaires and CNRS UMR 6047, 75015 Paris, France

[3] Université de Paris, Institut Cochin, INSERM, CNRS, F-75014 Paris, France.

[4] Evotec, 40 Avenue Tony Garnier, 69007 Lyon, France.

[5] Institut Curie, PSL Research University, Centre de Recherche, CurieCoreTech Mass Spectrometry Proteomics, Paris 75248 Cedex 05, France.

[#] Lead contact.

[*] Correspondence: carmen.buchrieser@pasteur.fr (C. B.), lionel.navarro@ens.psl.eu (L. N.)

Abstract

RNA silencing is a gene silencing mechanism directed by siRNAs and miRNAs. Human miRNAs act as central regulators of host-bacteria interactions. However, it is unknown whether human pathogenic bacteria could impede RNA silencing to promote virulence. Here, we show that the *Legionella pneumophila* type IV-secreted effector LegK1 suppresses siRNA- and miRNA-activities in human cells. This ability depends on its kinase activity and on a functional tryptophan-dependent Argonaute (Ago)-binding platform. We further show that the capacity of LegK1 to activate NF-κB signaling contributes to silencing suppression, demonstrating a link between effector-mediated NF-κB signaling activation and silencing suppression. LegK1 also promotes *L. pneumophila* growth in both amoeba and human macrophages, supporting a key role of this effector in virulence. In infected macrophages, the latter activity relies on the genetic targeting of human Ago4, highlighting a novel function of this host factor in antibacterial resistance.

Introduction

Legionella pneumophila is a Gram-negative bacterium, which infects and replicates in freshwater amoebae and ciliated protozoa in the environment[1-4]. When contaminated water droplets are inhaled by humans, *L. pneumophila* incidentally infects lung alveolar macrophages, which can result in a severe form of pneumonia called Legionnaires' disease[4-5]. *L. pneumophila* has evolved a type IV secretion system, referred to as the Dot/Icm system, to promote pathogenesis[6-8]. This secretion system translocates over 330 effectors into host cells and is essential for the replication of *L.*

pneumophila in protozoan and in human macrophages[9-13]. A significant proportion of *L. pneumophila* effectors resembles eukaryotic-like proteins or encode eukaryotic domains, and has likely been co-opted for subverting host functions[13-16]. Among them, the family of LegK proteins comprises proteins encoding eukaryotic-like kinase domains targeting specific host proteins[15]. For example, LegK1 is a serine/threonine protein kinase that phosphorylates the NF-κB inhibitor IκBα, as well as other IκB and NF-κB family members, resulting in a potent NF-κB signaling activation in human cells[17]. This effector contributes to the sustained Dot/Icm-dependent NF-κB signaling detected during *L. pneumophila* infection of human alveolar macrophages[18-20]. Furthermore, it triggers the induction of anti-apoptotic and host cell survival genes[18-20], which is thought to promote *L. pneumophila* growth in human macrophages.

MicroRNAs (miRNAs) are small non-coding RNAs (sRNAs) that post-transcriptionally regulate genes through the targeting of sequence complementary mRNA targets. In mammals, the miRNA biogenesis pathway involves the cleavage of primary miRNA transcripts by the Drosha-DGCR8 complex, which further releases hairpin-based miRNA precursors that are subsequently processed by the RNAse III enzyme Dicer[21]. The resulting miRNA duplexes then bind to an Argonaute (Ago) protein, and one strand, the guide, remains associated to this silencing effector to form a miRNA-Induced Silencing Complex (miRISC)[22-23]. The miRISC further directs silencing of mRNA targets through endonucleolytic cleavage (slicer activity), translational repression and/or mRNA degradation[21-22,24]. Four structurally conserved Ago proteins (Ago1-4) are encoded by the human genome[25-26]. Human Ago2 is the most characterized Ago member that possesses a slicer activity directed by a catalytic tetrad, DEDH (Asp-Glu-Asp-His), embedded in its PIWI domain[27-30]. This factor is the

central component of the miRISC[31]. Mechanistically, the phosphorylation of Ago2 at serine 387 triggers its binding to trinucleotide repeat containing 6 (TNRC6) proteins, which are tryptophan (W)-rich cofactors that associate with the PIWI domain of Ago2 through W-repeats (W-motifs) found in their N-terminal Ago-binding domains (ABDs)[29,32-34]. These molecular events are essential for High Molecular Weight (HMW)-miRISC assembly by recruiting downstream effector proteins[22-23], including those involved in decapping (Decapping protein 1/2, DCP1/2), RNA unwinding (DEAD-Box RNA helicase 6, DDX6), and deadenylation (carbon catabolite repressor 4/ negative regulator of transcription, CCR4/NOT)[35-36]. In addition, TNRC6 proteins use W-motifs embedded in their C-terminal silencing domains to directly bind CCR4-NOT and PAN2-PAN3 (poly(A)-specific ribonuclease 2) deadenylase complexes, thereby contributing to HMW-miRISC activity[35,37-40]. This series of molecular events leads to the translational repression, destabilization and degradation of mRNA targets, and in turn regulates diverse biological processes, including development (*e.g.* neurological development), differentiation, stress signaling and antiviral responses[41-46]. Human Ago1 and Ago4 are slicer-deficient and thus trigger gene silencing through endonucleolytic-independent mechanisms[27,47]. In contrast, human Ago3 retains a canonical DEDH catalytic tetrad and was recently shown to trigger RNA cleavage when loaded with specific guide miRNAs, in particular 14-nt 3' end-shortened miRNA variants[48-49]. Although very little is known about the biological functions of these three Ago proteins, gene deletions of Ago1 and Ago3 have been retrieved in patients suffering from neurological disorders[50-51]. Furthermore, several biological functions have been ascribed to mammalian Ago4. This factor has been shown to (i) regulate meiotic entry and meiotic sex chromosome inactivation in mice germ cells[52], (ii) translationally inhibit the second cistron of the *CACNA1A* locus in a miRNA-dependent

manner, thereby inhibiting the growth of neurons and Purkinje cells in mice[53], (iii) interact with the *de novo* methyltransferase DNMT3A and in turn direct cytosine methylation of some mature miRNAs, which inhibits their functions and is associated with poor prognosis in glioma[54], (iv) mediate RNA-dependent DNA methylation in human cells[55], and (v) promote antiviral resistance in mice[56]. Therefore, despite early assumptions that mammalian Ago proteins function redundantly, they can also exhibit very specialized functions.

Human miRNAs have been extensively studied in the context of host-bacteria interactions[57]. They regulate various cellular processes during bacterial infection, including innate immune responses, host cell cycle, cell death and survival pathways, autophagy, and cytoskeleton organization[57]. For example, *L. pneumophila* triggers the differential expression of 85 human miRNAs during infection of macrophages[58]. Among them, miR146a was found up-regulated and required to restrict the growth of *L. pneumophila* in human macrophages[58]. Furthermore, a trio of down-regulated miRNAs, namely miR-125b, miR-221 and miR-579, was shown to target repressors of *L. pneumophila* replication in macrophages[58]. Interestingly, *L. pneumophila* infection is not only modulating the expression of human miRNAs, but *L. pneumophila* is itself translocating active small RNAs (sRNAs) *via* extracellular vesicles (EVs) into the host cell[59]. Indeed, 15 sRNAs were identified that mimic human miRNAs and two of these, namely RsmY and tRNA-Phe, down-regulate selected sensor and regulator proteins of the host innate immune response in a miRNA-like manner[59]. Intriguingly, a recent study also shows that human airway cells make use of EVs to deliver let-7b-5p into *Pseudomonas aeruginosa* and reprogram bacterial gene expression, thereby reducing biofilm formation and antibiotic resistance[60]. Altogether, these studies, among many

others, highlight a central role played by sRNAs in the reprogramming of both host and bacterial gene expression during infections.

Although the role of human miRNAs in host-bacteria interactions is now well-established, there is currently no evidence indicating that human pathogenic bacteria can interfere with RNA silencing as part of their virulence functions. This has, however, been previously characterized in a phytopathogenic *Pseudomonas syringae* strain, which delivers several type III-secreted effectors into the host cell to suppress different steps of the Arabidopsis miRNA pathway[61]. It has also been extensively characterized in mammalian viruses that produce Viral Suppressors of RNA silencing (VSRs) to replicate in host cells[43-44,62-64]. In this study, we found that the *L. pneumophila* type IV-secreted effector LegK1 acts as a *bona fide* Bacterial Suppressor of RNA silencing (BSR). We show that LegK1 efficiently suppresses siRNA- and miRNA- activities in human cells through both its kinase activity and a functional Ago-binding platform. We further demonstrate that the ability of LegK1 to activate NF-κB signaling contributes to silencing suppression. In addition, we found that LegK1 promotes *L. pneumophila* growth in both human macrophages and amoeba, supporting a virulence function of this effector in biologically relevant host cells. Importantly, the genetic targeting of human Ago4 by LegK1 was found required to promote *L. pneumophila* growth in macrophages. Therefore, besides identifying the first BSR from a pathogenic bacterium, this study unveils an unexpected link between effector-mediated NF-κB signaling activation and silencing suppression, as well as a novel function of human Ago4 in host-bacteria interactions.

Results

The *L. pneumophila* effector LegK1 suppresses siRNA-directed silencing in human cells

The known Ago-binding function of W-motifs, present in some endogenous silencing factors as well as in some VSRs[62,65-69], prompted us to examine whether effectors from human pathogenic bacteria have also evolved such Ago-binding platforms to interfere with RNA silencing. To test this hypothesis, we retrieved the protein sequences from 25 genomes of pathogenic bacteria and used them to the Wsearch algorithm to search for putative W-motifs[70] (Figure S1a). The score of each W-motif was determined using the animal Bidirectional Position-Specific Scoring Matrix (BPSSM), generated from experimentally-verified Ago-binding proteins and their orthologous sequences[70]. Among the candidate proteins exhibiting the highest W-score, we selected a subset of secreted virulence factors and tested their possible effects on the siRNA-based *CXCR4* reporter[71] (Figure S1b). This reporter system relies on the co-transfection of two plasmids along with exogenous siRNAs targeting the 3'UTR of *CXCR4*. The first plasmid expresses the *firefly luciferase* fused to the 3'UTR of *CXCR4*, while the second one expresses the *renilla luciferase*, which served as a transfection control. We first showed that the silencing of the *luciferase* reporter was compromised in the *ago2*$^{-/-}$ and *ago1*$^{-/-}$/*ago2*$^{-/-}$ CRISPR/Cas9-based mutant HeLa cell lines, as revealed by an increased luminescence intensity compared to control cells (Figure S1c, d). In contrast, the silencing of the *luciferase* remained effective in *ago1*$^{-/-}$ and *dicer*$^{-/-}$ cell lines (Figure S1c, d). Collectively, these results indicate that the *CXCR4* reporter system is dependent on Ago2, but not on Ago1. They also indicate that Dicer is not required for this process, which is consistent with the exogenous

delivery of mature anti-*CXCR4* siRNAs. Significantly, when monitoring luminescence intensity in HeLa cells expressing individually these 8 candidate bacterial W-effectors (Figure S1e-g), we found that LegK1 from *Legionella pneumophila* (strain Paris) was the sole effector capable of inhibiting the silencing of the *CXCR4* reporter, as found in *ago2*$^{-/-}$ cells or in cells expressing the VSR *Hepatitis B virus* HBx[72] (Figure S1h, i). Altogether, these data indicate that LegK1 suppresses the silencing of an Ago2-dependent siRNA-based reporter system.

LegK1 suppresses siRNA- and miRNA-directed gene silencing through both its kinase activity and a predicted tryptophan-dependent Ago-binding platform

LegK1 is an experimentally validated Dot/Icm type IV-secreted effector possessing a eukaryotic-like serine/threonine kinase activity[17]. Here, we additionally found that LegK1 contains a putative Ago-binding platform composed of four predicted W-motifs (Figure S1j). The tryptophan residues located at positions 41, 283 and 293 of the LegK1 protein sequence, namely W41, W283 and W293, displayed the highest W-score, and were thus selected for further analyses (Figures 1a and S1j). We first substituted each of these three tryptophans by phenylalanine (W>F; LegK1-3WF). In parallel, we generated a K121A substitution in the LegK1 ATP-binding site (LegK1-KA), which has been previously shown to abolish the kinase activity of this effector[17]. Both LegK1-3WF and LegK1-KA proteins accumulated to the same levels as wild-type (WT) LegK1 proteins in HEK293T cells (Figure 1b), indicating that these mutated proteins are stable when expressed in human cells. We further analyzed their ability to suppress RNA silencing. To this end, we used a siRNA-based *GFP* reporter system, which relies on the co-transfection of a plasmid expressing the *enhanced GFP* (*eGFP*),

together with anti-*GFP* siRNAs targeting a single site located in the 5' region of the *eGFP* coding sequence. This siRNA-based reporter system has been previously used to characterize VSRs from different human pathogenic viruses[73-74]. We found that this reporter was robustly silenced by the anti-*GFP* siRNAs, as revealed by low accumulation of eGFP proteins when expressed in HeLa and HEK293T cells (Figure 1c-e). In contrast, the eGFP protein accumulation was moderately increased in the *ago2*$^{-/-}$ HeLa cell line expressing the anti-*GFP* siRNA duplexes, an effect which was found enhanced in the *ago1*$^{-/-}$/*ago2*$^{-/-}$ mutant cells (Figure 1c). These results indicate that both Ago1 and Ago2 proteins direct the silencing of this reporter system. Of note, the fact that the reporter was not fully derepressed in *ago1*$^{-/-}$/*ago2*$^{-/-}$ HeLa cells suggests that Ago3 and/or Ago4 must additionally contribute to its silencing. When the same analysis was conducted in HEK293T cells expressing LegK1, we found an efficient suppression of *eGFP* silencing, a process which was not observed in cells expressing the empty vector or the type III-secreted YopM effector from *Yersinia pestis*, which is deprived of silencing suppression activity (Figure 1d, e). It is noteworthy that the silencing suppression effect mediated by LegK1 was even more pronounced than the one triggered by T6B, a TNRC6B-derived peptide containing multiple W-motifs, which was shown to disrupt the function of multiple Ago proteins[75] (Figure 1e). Taken together, these data indicate that LegK1 efficiently suppresses the silencing of an siRNA-based reporter controlled by multiple Ago proteins. Importantly, we found that the LegK1-3WF and LegK1-KA mutant versions no longer triggered silencing suppression of this siRNA-based GFP reporter (Figure 1e). Therefore, both the kinase activity and the putative Ago-binding platform of LegK1 are essential for the silencing suppression of this reporter.

To investigate whether LegK1 additionally suppress miRNA functions, we made use of a previously characterized *GFP*-based construct that contains two artificial miRNA precursors embedded in an intron sequence located upstream of the GFP coding sequence[76]. This construct produces two mature anti-*GFP* miRNAs, which are perfectly complementary to the *GFP* mRNA sequence[76]. These artificial miRNAs were previously shown to trigger the self-silencing of the *GFP* reporter in a Drosha- and DGCR8-dependent manner[76]. Using this reporter system, we show that LegK1 triggers an increased GFP protein level compared to cells expressing the control effector YopM (Figure 1f, g). This was, however, not the case in response to T6B, suggesting that the Ago-binding activity of this peptide does not sufficiently alter the function(s) of the Ago protein(s) that silence(s) this reporter (Figure 1g). Therefore, unlike T6B, LegK1 can suppress miRNA-directed silencing of this *GFP*-based reporter. In contrast, the GFP protein levels remained low in HEK293T cells expressing LegK1-KA and LegK1-3WF mutants (Figure 1g), indicating that these mutants no longer suppress miRNA activity. Altogether, these data reveal that LegK1 can efficiently suppress siRNA- and miRNA-activities through both its kinase activity and a predicted W-dependent Ago-binding platform.

LegK1 interacts with RISC factors, including Ago2 and its PIWI domain

The presence of predicted W-motifs in the protein sequence of LegK1 and their relevance in silencing suppression, suggested that this effector could interact with human Ago proteins. To test this possibility, we expressed the Flag-tagged LegK1-WT, LegK1-KA and LegK1-3WF versions in HEK293T cells and immunoprecipitated their cellular partners. Using Western blot analysis, we demonstrated that Ago1, Ago2 and Ago4 proteins were recovered from Flag-LegK1 immunoprecipitates, which was

not observed after immunoprecipitation of Flag-eGFP from control cells (Figure 2a, b). This result indicates that LegK1 interacts with protein complexes containing Ago1, Ago2 and Ago4 proteins. Interestingly, we also recovered in the Flag-LegK1 immunoprecipitates the TNRC6A, PABPC1 and DDX6 proteins, which are well-characterized HMW-miRISC factors[35-36,77-79], suggesting that LegK1 interacts with mature Ago-RISCs engaged in RNA target repression. Importantly, the above interactions were maintained with the catalytic mutant LegK1-KA, while they were significantly reduced with the LegK1-3WF mutant (Figure 2a, b). These data suggest that the Ago-binding platform of LegK1 is required to interact with Ago-RISCs, while its kinase activity is dispensable for this process. Furthermore, we found that RNAse A treatment did not alter the ability of Flag-LegK1 to interact with GFP-Ago2 (Figure 2c). LegK1 thus interacts with human Ago2 in an RNA-independent manner.

We next investigated whether LegK1 directly interacts with human Ago2. For this end, we conducted an *in vitro* interaction assay using GST-Ago2 and His_6-SUMO-LegK1$^{2:386}$ –deprived of its predicted transmembrane domain–, which were both expressed and purified from *E. coli* (Figure 2d, e). We found that the GST-tagged Ago2 protein efficiently bound to His_6-SUMO-LegK1$^{2:386}$, while it did not interact with the TAP negative control (Figure 2e). Because the PIWI domain of human Ago2 is known to possess W-binding interfaces[32,80-82], we additionally expressed and purified a CBP-tagged PIWI domain of human Ago2 (Figure 2d, f). Using an *in vitro* pull-down assay, we found that the CBP-PIWI$^{517:859}$-His_6 recombinant protein interacted with His_6-SUMO-LegK1$^{2:386}$, however this interaction was not further improved in the presence of RNA extracts from HEK293T cells (Figure 2f). Therefore, we show that LegK1 directly interacts with human Ago2 likely through interaction surfaces embedded in its

PIWI domain. Our data also suggest that one or several W-motifs of LegK1 orchestrate the interaction between this bacterial effector and human Ago proteins.

The two W-motifs embedded in the kinase domain of LegK1 exhibit binding capacity to human Ago proteins

To further examine the contribution of the selected W-motifs of LegK1 in Ago-binding, we first attempted to express and purify the LegK1-3WF mutant version from *E. coli*. However, this mutant formed insoluble inclusion bodies, preventing further *in vitro* pull-down experiments (Figure S2). To circumvent this issue, we next chemically synthesized biotinylated peptides containing each candidate W-motif (W41, W283 and W293), surrounded by native amino acid residues, referred to here as W1, W2 and W3 peptides (Figure 3a). In parallel, we synthetized identical peptides where each tryptophan was substituted by phenylalanine, named F1, F2 and F3 mutant peptides. A pull-down experiment of each individual peptide was performed to elute bound proteins. Using this approach, we found that the W1 peptide did not bind to any of the Ago proteins, indicating that W41 is not a functional Ago-binding motif (Figure 3b). In contrast, the W2 and W3 peptides exhibited a clear binding to human Ago1, Ago2, Ago3 and Ago4, but not to the negative control GAPDH (Figure 3b, c). Therefore, the W2 and W3 peptides can interact with the four Ago proteins. Interestingly, the binding to these Ago proteins was lost in the presence of the F2 peptide, providing evidence that the W283 residue is a functional Ago-binding motif (Figure 3b). The F3 mutant peptides remained, however, competent in interacting with the four Ago proteins (Figure 3b). To assess whether the W293 residue is functional, we further synthesized a peptide carrying a substitution of the tryptophan residue into alanine (Figure 3a), a point mutation that has been the most extensively used on W-rich proteins to alter

Ago-binding[32,65,80-81,83]. Indeed, the resulting A3 peptide no longer interacted with Ago proteins (Figure 3c), supporting a key role for the W293 motif in the interaction with human Ago proteins. Collectively, these data indicate that both the W283 and W293 motifs, which are embedded in the kinase domain of LegK1, behave as canonical Ago-binding motifs.

The W283 and W293 motifs of LegK1 and their surrounding residues exhibit sequence conservation among *Legionella* species

To get some insights into the sequence conservation of the W-motifs of LegK1, we retrieved and aligned the protein sequences of putative LegK1 homologs from the *Legionella* protein sequences available on the National Center for Biotechnology Information (NCBI). More specifically, we selected for this analysis LegK1 homologous protein sequences exhibiting a protein identity of at least 40% to the *L. pneumophila* LegK1 strain Paris. According to these criteria, LegK1 was found present in 15 other *Legionella* species[4,13] (Figure 3d). Although the W41 motif was found conserved among all the *Legionella* species analysed, its surrounding residues were highly variable (Figure 3d). Furthermore, they did not fulfill the typical features of residues neighbouring functional W-motifs, which are composed of small, polar and non-hydrophobic residues[70]. This observation is thus consistent with our experimental data indicating that this Ago-binding motif is not functional (Figure 3b). In contrast, the W293 motif of the strain *L. pneumophila* Paris, and its surrounding residues, were conserved among all *Legionella* species analysed (Figure 3d). The equivalent W293 motifs present in the different LegK1 homologous protein sequences analysed here thus probably maintain their Ago-binding capacity. When we analysed the sequence conservation of the W283 motif, and its surrounding residues, we found that these

amino acids were also conserved among a cluster including *L. pneumophila*, *L. norrlandica* and *L. waltersii* (Figure 3d, blue clade). However, we noticed sequence variations in the remaining *Legionella* species analysed, which were not only found in the surrounding residues, but also in the tryptophan itself (tryptophan to tyrosine residues (W>Y); Figure 3d). Given that a tyrosine is one of the least probable residues that forms a functional W-motif[70], this observation suggested that the equivalent W283 motifs from these *Legionella* LegK1 protein sequences had lost, or alternatively never gained, the ability to bind Ago proteins. Consistent with this hypothesis, a biotinylated peptide corresponding to the region of the *L. quateirensis* LegK1 sequence carrying the W>Y natural variation, named Y2, did not bind to any of the human Ago proteins (Figure 3e, f). Therefore, the equivalent W283 motifs from LegK1 homologs should be functional in *L. norrlandica* and *L. waltersii,* but not in the remaining *Legionella* species.

Concomitant mutations in the two functional W-motifs of LegK1 abolish the ability of this effector to phosphorylate IκBα and to suppress RNA silencing

The fact that the two functional W-motifs are embedded in the kinase domain of LegK1 prompted us to further investigate the relationship between the Ago-binding platform and the kinase activity of this effector. To this end, we examined the possible impact of single and concomitant W-motif mutations on the ability of LegK1 to phosphorylate IκBα, a known substrate of this effector protein[17]. More specifically, we expressed the WT or the mutant versions of LegK1 in HEK293T cells, and further incubated the immunoprecipitates from each cell lysate with purified recombinant CBP-IκBα-His_6. Western blot analyses from these cell-free extracts, using an antibody recognizing phosphorylation at Ser-32 of IκBα, revealed strong LegK1-induced phosphorylation of

CBP-IκBα-His$_6$ (Figures 4a and S3). While the single LegK1-W283F and LegK1-W293F mutants triggered comparable phosphorylation levels at Ser-32 of IκBα, the LegK1-W293A mutant was partially compromised in this process (Figure 4a). Importantly, the phosphorylation at Ser-32 of IκBα was fully abolished in the presence of LegK1-W283F-W293A, despite the stable accumulation of this double mutant in HEK293T cells (Figure 4a). These effects were similar to the ones detected with the LegK1-3WF and the LegK1-KA mutants (Figure S3). Therefore, the concomitant mutations in the two functional W-motifs of LegK1 are sufficient to abolish its catalytic activity.

We next assessed the possible impact of these W-motif mutations on the silencing suppression activity of LegK1 using the siRNA-based *GFP* reporter in HEK293T cells. We found that the LegK1-W293A mutant, and particularly the LegK1-W283F-W293A double mutant, were altered in their ability to suppress siRNA-guided silencing, as revealed by an impaired GFP derepression (Figure 4b). These effects were comparable to the ones observed in HEK293T cells expressing YopM, LegK1-3WF or LegK1-KA mutants (Figure 1e). We conclude that the W293 motif has a major role in LegK1-triggered silencing suppression and that both the W283 and W293 motifs must cooperatively orchestrate this process. Altogether, these data indicate that the kinase, Ago-binding and RNA silencing suppression activities of LegK1 are tightly interconnected.

LegK1-triggered NF-κB signaling activation contributes to RNA silencing suppression

Given that the kinase and silencing suppression activities of LegK1 were found to be interconnected, we reasoned that LegK1 could directly phosphorylate human Ago proteins to alter their functions. To test this hypothesis, we investigated whether LegK1 could phosphorylate human Ago2. Nevertheless, we did not observe any increase in the phosphorylation status of the human Ago2 protein in the presence of LegK1 (Figure S3, Supplementary text), indicating that LegK1 unlikely phosphorylate this host factor. Instead, these results suggest that LegK1 could suppress RNA silencing by phosphorylating other RISC component(s) and/or proteins that indirectly regulate RNA silencing activity. Because LegK1 has been shown to directly phosphorylate IκBα, resulting in a potent NF-κB signaling activation[17] (Ge *et al*., 2009), and because its catalytic activity was found here to be essential for RNA silencing suppression (Figure 1e, g), we further investigated whether LegK1-triggered NF-κB signaling activation could contribute to silencing suppression. For this purpose, we tested if the Caffeic Acid Phenethyl Ester (CAPE), a well-established NF-κB signaling inhibitor[84-85], could alter the ability of LegK1 to suppress silencing of the siRNA-based *GFP* reporter in HEK293T cells. Interestingly, while LegK1 triggered a significant derepression of siRNA-directed silencing of the *GFP* reporter compared to the control vector, we found that this effect was significantly reduced upon CAPE treatment, which concomitantly prevented LegK1-induced phosphorylation at Ser-32 of IκBα (Figure 4c). Of note, the low GFP protein accumulation detected in this condition was not due to a destabilization of the GFP in response to CAPE, because a normal GFP protein level was observed upon CAPE treatment of HEK293T cells expressing LegK1 and control

siRNAs (Figure 4c). The CAPE-dependent suppression of NF-κB signaling can thus restore the ability of siRNAs to silence the *GFP* reporter in the presence of LegK1. Collectively, these results demonstrate that the silencing suppression activity of LegK1 is in part achieved through activation of NF-κB signaling directed by its kinase activity.

LegK1 promotes the growth of *L. pneumophila* in both *Acanthamoeba castellanii* and human macrophages

To determine whether LegK1 contributes to the virulence of *L. pneumophila*, we first generated an isogenic *legK1* deletion mutant, referred to here as the *Lpp* Δ*legK1* strain. Whole-genome sequencing of *Lpp* Δ*legK1* confirmed a unique deletion in the *legK1* gene, which did not affect the fitness of this bacterium *in vitro* (Figure S4a, b). We next infected *Acanthamoeba castellanii,* a natural host of *L. pneumophila*, with the *L. pneumophila* WT and Δ*legK1* strains and further monitored bacterial numbers during the course of the infection. Interestingly, the growth of the *Lpp* Δ*legK1* strain was reduced in *A. castellanii* compared to that of *L. pneumophila* WT (Figure 5a). Because *L. pneumophila* can accidentally infect humans where it replicates in alveolar macrophages, we conducted the same assay in macrophages derived from THP-1 cells. Similarly, a reduced intracellular replication of the Δ*legK1* strain was observed compared to the one achieved by the WT strain (Figure 5b). These growth defects were partially complemented in both *A. castellanii* and human macrophages, respectively, when LegK1 was expressed *in trans* in the *Lpp* Δ*legK1* strain (Figure 5c, d). These data indicate that the reduced growth of *Lpp* Δ*legK1* in both *A. castellanii* and human macrophages is due to the deletion of *legK1*. They also provide evidence

that LegK1 is a major virulence factor of *L. pneumophila* that promotes bacterial growth in both amoeba and human macrophages.

Human Ago4 is a functionally relevant genetic target of LegK1 in infected macrophages

We next analysed whether LegK1 genetically targets human Ago functions to promote *L. pneumophila* virulence. Using available RNA-seq datasets[86], we first noticed that human *Ago2* and *Ago4* mRNAs were the most abundant *Ago* transcripts in THP-1 cells (Figure 5e). This analysis supports recent findings showing that *Ago4* is highly expressed in immune-related cells[56]. Consistently, we detected a higher Ago4 protein accumulation in THP-1 cells compared to HEK293T and A549 epithelial cells, which was also detected for Ago2, albeit to a lesser extent (Figure 5f). Based on these data, we decided to knock-out human Ago2 or Ago4 in THP-1 cells for further functional assays. A single guide RNA approach was used to generate CRISPR/Cas9-based deletions in the second exon of the Ago2 and in the third exon of the Ago4 loci. The resulting pools of *ago2*$^{-/-}$ and *ago4*$^{-/-}$ THP-1 lines were found respectively deprived of Ago2 and Ago4 proteins compared to THP-1 control cells (Figure 5g). Macrophages derived from the *ago2*$^{-/-}$ and *ago4*$^{-/-}$ THP-1 cells were infected with the *L. pneumophila* WT or Δ*legK1* strains and bacterial numbers were monitored at 24 *hpi*. A normal growth of the WT strain was achieved in *ago2*$^{-/-}$ and *ago4*$^{-/-}$ cells compared to control cells (Figure S4c), indicating that neither human Ago2 nor Ago4 control the growth of this bacterium in those conditions. Importantly, however, the growth defect of the *Lpp* Δ*legK1* strain was partially rescued in *ago4*$^{-/-}$ macrophages (Figure 5g), indicating that the lack of Ago4 facilitates the growth of this bacterial mutant in macrophages. The

latter rescue experiment demonstrates that human Ago4 is a functionally relevant genetic target of LegK1 in infected macrophages.

Discussion

Here, we showed that the type IV-secreted protein LegK1 from *L. pneumophila* can efficiently suppress RNA silencing in human cells (Figures 1 and 2, Figure S1). More specifically, LegK1 dampened the silencing of the Ago2-dependent siRNA-based *CXCR4* reporter (Figure 1). It also suppressed the silencing of a siRNA-based *GFP* reporter system, which depends, at least in part, on human Ago1 and Ago2 (Figure 1). In addition, we found that LegK1 was able to efficiently suppress a miRNA-based *GFP* reporter system (Figure 1). Importantly, these silencing suppression effects relied on a W-dependent Ago-binding platform, which was critical for the interaction of LegK1 with human Ago proteins (Figures 1, 2). Thus, these data indicate that LegK1 acts as a *bona fide* BSR by suppressing both siRNA- and miRNA-activities in human cells through a functional Ago-binding platform. The use of such Ago-binding platform is therefore not restricted to VSRs, as previously thought[62,66-67], but can be additionally exploited by at least one human pathogenic bacterium.

LegK1 was not only capable to bind human Ago1, Ago2 and Ago4 through its W-motifs, but was also recovered in protein complexes composed of TNRC6A, PABPC1 and DDX6 (Figure 2). Because these factors are part of the HMW-miRISC[22-23], our data suggest that LegK1 interferes with the function of mature RISCs that are engaged in the silencing of sRNA targets. Intriguingly, we also noticed that the WS and LWG residues, which are present in the C-terminal domain of TNRC6 proteins, and known

to be required for the direct interaction with components of deadenylase complexes[35,37-40], are also part of the W283 (DVWSTG) and the W293 (LWGD) motifs of LegK1. These observations suggest that LegK1 might additionally use its W-motifs to physically interact with deadenylase complexes. This hypothesis is consistent with our co-immunoprecipitation data showing that LegK1 interacts with DDX6, a direct partner of CNOT1[35,78]. Based on these data, we propose that LegK1 might trigger silencing suppression by altering, at least in part, the function of HMW-RISCs. Such a mode of action would be well-adapted to rapidly repress RNA targets that fine-tune innate immune responses during *L. pneumophila* infections[58]. It would also be analogous to the mode of action of the *Sweet potato mild mottle virus* (SPMMV) VSR P1, which was shown to interact with *Nicotiana benthamiana* AGO1 through W-motifs and to co-fractionate with RISC containing AGO1-loaded small RNAs[67] (Giner *et al*., 2010).

We also found that the two W-motifs from the kinase domain of LegK1, namely W283 and W293, are essential for the binding of LegK1 to human Ago proteins (Figure 3). Interestingly, these tryptophan residues were found interspaced by 9 amino acids, which is a typical feature of functional W-motifs embedded in the ABD of TNRC6 proteins, which are in most cases separated by 8 to 14 amino acids from each other[29-30,49]. This amino acid organization is thought to form a flexible linker that facilitates the interaction of W-motifs with the three W-binding pockets exposed at the surface of human Ago2 and Ago4 proteins, which are separated by a distance of 25 Å from each other[29-30,48]. Based on these findings, we propose that the W283 and W293 motifs of LegK1 cooperate with each other to ensure a tight association between this bacterial protein and the W-binding pockets of human Ago proteins. It is also noteworthy that

these W-motifs are not positioned in a disordered region, such as the ones typically found in the ABDs of TNRC6 proteins[32,65,81-82,87]. Instead, they are embedded in a structured kinase domain. Our data therefore imply to revisit *in silico* predictions of Ago-binding platforms located in structured domains, which were so far discarded from experimental validations[70].

To get further insights into the functional relevance of the W283 and W293 motifs of LegK1 in Ago-binding, we analyzed their sequence conservation across *Legionella* species. We found that the region corresponding to the *L. pneumophila* W293 motif, and its surrounding residues, are conserved among several *Legionella* species. The region corresponding to the W283 motif was also found conserved in *L. norrlandica* and *L. waltersii* species. In contrast, amino acid sequence variations were observed in the tryptophan and surrounding residues of the LegK1 protein sequences derived from the remaining analysed *Legionella* species. Furthermore, they prevented Ago-binding of a peptide derived from the *L. quateirensis* LegK1 protein sequence (Figure 3). Therefore, the conservation of the W283 and W293 motifs, observed in some *Legionella* species, supports our experimental data showing that these W-motifs likely cooperate between each other to form a functional Ago-binding platform.

By disabling the two functional W-motifs from the Ago-binding platform of LegK1, we found that this effector was fully compromised in its ability to phosphorylate IκBα and to suppress RNA silencing (Figure 4). These data are consistent with the central role played by the kinase activity of LegK1 in RNA silencing suppression (Figure 1), and support a tight interconnection between the kinase and Ago-binding activities of LegK1. In addition, we discovered that the blockage of NF-κB signaling activation in

human cells expressing LegK1 reduced the siRNA-directed silencing of the *GFP* reporter system (Figure 4). These data unveil an unexpected cross-talk between LegK1-mediated activation of NF-κB signaling and silencing suppression. They also highlight an interconnection between the kinase, RNA silencing suppression and NF-κB signaling activation activities of LegK1, which remains to be characterized in more depth in the future. It will notably be important to assess if cellular pools of human Ago proteins could be recovered in protein complexes containing NF-κB-related factors, and whether LegK1 acts on specific components of such complexes, besides IκBα and Ago proteins, to suppress RNA silencing while enhancing NF-κB signaling.

The long-lasting coevolution of *Legionella* in a wide range of amoebae and ciliated protozoa has shaped the *Legionella* genomes[9,13]. The presence of a large repertoire of eukaryotic-like proteins in the *Legionella* genomes indicates that these proteins must have been acquired through horizontal gene transfer from protist host organisms[13-16,88]. Accordingly, most of the virulence strategies used by *L. pneumophila* are required to replicate in both protists and human macrophages[4-5]. Consistently, we showed that the *Lpp ΔlegK1* strain was altered in its ability to replicate in both *A. castellanii* and human macrophages (Figure 5), supporting a physiologically relevant role of LegK1 in *L. pneumophila* virulence. In addition, we found that the growth defect of the *Lpp ΔlegK1* strain was partially rescued in Ago4-deficient human macrophages, (Figure 5). This finding suggests that the targeting of Ago proteins by LegK1 is likely a major virulence function of this effector, which might also be required to promote growth of *L. pneumophila* in its natural hosts. This assumption is supported by the fact that amoebae genomes like *Dictyostelium discoideum*, possess canonical Ago proteins, some of which are even experimentally characterized in RNA silencing[89].

Here, by searching for the presence of Ago-like factors in the recently released genome sequence of the *A. castellanii* strain used in this study[90], we recovered two candidate Ago-like proteins composed of canonical PIWI and PAZ domains (Figure S4d). In contrast, none of the NF-κB-related domains were retrieved from the genomes of amoebae, including the *A. castellanii* strain used herein[5,90]. Based on the lack of NF-κB-related genes in amoebae genomes, and on the presence of canonical Ago proteins in these natural hosts, we propose that the ability of LegK1 to suppress Ago activities is likely the primary virulence function of this bacterial effector.

Antiviral RNA interference (RNAi) has been extensively characterized in plants, fungi, insects and worms[91-95]. In mammals, emerging evidence indicates that antiviral RNAi also operates in embryonic stem cells, adult stem cells and progenitor cells, in which the antiviral interferon (IFN) response –known to repress RNAi– is less active[96-99]. In these tissues/cell types, canonical antiviral sRNAs readily accumulate during viral infections and inhibit viral replication in an Ago2-dependent manner[43-44,98]. Interestingly, mouse Ago4 was also recently shown to restrict the replication of different viruses in IFN-competent cells, including *influenza A virus* (IAV)[56]. Importantly, mouse Ago4 was also shown to dampen IAV replication *in vivo*, further supporting a key role of this factor in antiviral resistance[56]. In the present study, we unveiled a novel function of human Ago4 in host-bacterial interactions. We first showed that Ago4 –and Ago2 to a lesser extent– were the most expressed Ago genes in immune-related cells (Figure 5). Significantly, although a normal growth of the *Lpp* WT strain was observed in human *ago2*$^{-/-}$ and *ago4*$^{-/-}$ macrophages, we found that the growth defect of the *Lpp* Δ*legK1* mutant was partially rescued in Ago4-deficient cells (Figure 5). This provides genetic evidence that LegK1 must suppress the function of

Ago4 to promote growth of *L. pneumophila* in IFN-competent macrophages. These findings therefore extend the roles of human Ago4 to antibacterial defense. They are thus consistent with previous reports in plants showing that AGO1 and AGO2 proteins orchestrate antibacterial defense, beyond their well-described antiviral functions[100-103].

In conclusion, this study reports on the first bacterial effector that directly suppresses RNA silencing by physically interacting with Ago proteins through W-motifs. Intriguingly, we have also retrieved W-motifs in an appropriate sequence context in effectors from various human pathogenic bacteria, fungi and parasites (Figure S5). These observations suggest that a wide range of non-viral mammalian pathogens and parasites might have evolved an analogous mode of action to promote virulence. It will thus be interesting to establish if the discoveries made on LegK1 hold true for other virulence/parasitic factors from non-viral mammalian pathogens/parasites. It will also be worth developing innovative strategies to counteract this potentially widespread virulence mechanism in order to control infectious and parasitic diseases.

Methods

Human cell lines and culture

HeLa cells (ATCC® CCL-2™), control (CTL), *ago1*$^{-/-}$, *ago2*$^{-/-}$, *ago1*$^{-/-}$/*ago2*$^{-/-}$ and *dicer*$^{-/-}$ CRISPR/Cas9-based HeLa cell lines[104] (this study), and Human Embryonic Kidney 293T cells (HEK293T) cells (ATCC® CRL-3216™) were cultured in high glucose Dulbecco's modified Eagle's medium (DMEM) (containing 4.5 g/l of glucose) (Dominique Dutscher, L0103-500). CTL and *ago2*$^{-/-}$ CRISPR/Cas9-based HeLa cell lines were previously generated[104]. LentiCRISPRv2-Ago1 and LentiCRISPRv2-Dicer expression plasmids expressing single-guide RNA targeting exon 3 of Ago1

(AAACTCATACACAGGCTTGCGATC) or Dicer (AAACCTGATCTGATAGGACAGCTC) genes respectively, were used to transfect HEK293T cells using Lipofectamine LTX (Life technologies, A12621). Forty-eight hours later, viral particles were harvested and used to transduce HeLa cells. Cells were selected in medium supplemented with puromycin for 15 days. Data acquisition and data analysis were performed on the Cochin Cytometry and Immunobiology core Facilities. Single cells were isolated from lentiCRISPRv2-Ago1 or lentiCRISPRv2-Dicer transduced cells using a BD Biosciences FACSAria III. Expression of Ago1 or Dicer in the cell clones was analyzed by SDS-PAGE and immunoblotting. One cell clone knockout was selected for further analysis. A549 cells (ATCC® CCL-185) were cultured in Ham's F-12K Nutrient Mixture (Kaighn's Modification) (Corning, 10-025-CVR). THP-1 (ATCC® TIB-202™) and THP-1 *ago2*$^{-/-}$ and *ago4*$^{-/-}$ cell pools (Synthego®, this study) were cultured in Gibco Roswell Park Memorial Institute (RPMI) 1640 medium (Dominique Dutscher, L0498-500). The percentages of editing efficiency after expansion were of 97% and 96% for THP-1 *ago2*$^{-/-}$ and *ago4*$^{-/-}$ cell pools, respectively. All media were supplemented with 10% fetal bovine serum. Cells were maintained at 37°C in a humidified 5% CO_2 atmosphere. In addition, all human cell lines were regularly tested negative for mycoplasma contamination.

***Acanthamoeba castellanii* culture**

Acanthamoeba castellanii (ATCC® 50739) was cultured in PYG 712 medium (2% proteose peptone, 0.1% yeast extract, 0.1 M glucose, 4 mM $MgSO_4$, 0.4 M $CaCl_2$, 0.1% sodium citrate dihydrate, 0.05 mM Fe $(NH_4)_2(SO_4)_2$ x $6H_2O$, 2.5 mM NaH_2PO_3, 2.5 mM K_2HPO_3) at 20°C for 72 h prior to harvesting for *L. pneumophila* infection.

Bacterial strains and mutant constructions

Legionella pneumophila strain Paris WT (CIP 107629T) and *ΔlegK1* (*Δlpp1439*) mutant were cultured in N-(2-acetamido)-2-aminoethanesulfonic acid (ACES)-buffered yeast extract broth (BCY) or on ACES-buffered charcoal-yeast (BCYE) extract agar[105]. When needed antibiotics were added: for *L. pneumophila*: gentamycin 12.5 µg/ml, chloramphenicol 10 µg/ml. All strains were grown at 37°C. The *ΔlegK1* mutant was constructed by replacing the gene of interest with a gentamycin resistance cassette in the chromosome. The mutant allele was constructed using a three-step PCR technique[106] (Table S1). Briefly, the gene of interest was inactivated by introduction of a gentamycin resistance cassette into the chromosome. Therefore, three overlapping fragments, corresponding to the upstream region, the antibiotic cassette and the downstream region of the gene of interest, were amplified independently and purified on agarose gels. The three resulting PCR products were mixed at the same molar concentration (15 nM) and a second PCR with flanking primer pairs was performed. The resulting PCR product, the gentamycin resistance cassette flanked by 500 bp regions homologous to *legK1* was introduced into *L. pneumophila* by natural competence for chromosomal recombination. Strains that had undergone allelic exchange were selected by plating on BCYE containing gentamycin and the mutant was verified by PCR and whole genome sequencing. Bacterial growth assays were performed by seeding the indicated strains in wells of a microtiter plate (TPP) containing 200µl of BYE. The microtiter plate was incubated with shaking at 37°C for 48 hours in a Tecan Infinte multiwell plate reader (Tecan Group). Optical density measurements were taken at 600nm every 30 min. For complementation, the *L. pneumophila* WT and *ΔlegK1* mutant strains were transformed by electroporation

(2.5kV, 200Ω and 25µF) with 100 ng of the empty plasmid or pBC-KS-LegK1. Transformants were selected by plating on BCYE containing chloramphenicol.

Expression plasmids and constructions

The expression vectors for bacterial candidates were generated using GATEWAY technology. Briefly, PCR amplification (Table S1) of *Lysteriolysin O* and *α-Hemolysin* coding sequences was performed using pAD-hly-Myc plasmid and *Staphylococcus aureus* SH1000 genomic DNA as templates, respectively (gift from Dr. Alice Lebreton, IBENS, Paris, France). *BepB* coding sequence was amplified from *Bartonella Henselae* gDNA, *ExoY* from *Pseudomonas aeruginosa* PAO1 strain, *NleH1* from *Escherichia coli* O157:H7 gDNA (gift from Dr. Julie Guignot, Institut Cochin, Paris, France), *Pertussis toxin* from *Bordetella pertussis* Tohama gDNA (gift from Dr. Benoit Garin, Institut Pasteur, Paris, France), *YopM* from *Yersinia pestis* gDNA (gift from Dr. Lauriane Quenee, Institute Biosafety Officer at Caltech, Los Angeles, USA). Finally, the coding sequence of *legK1* (*lpp1439*) was PCR amplified using gDNA of the *Legionella pneumophila* strain Paris. All resulting PCR products were introduced into the pENTR/D-TOPO entry vector (Invitrogen, K240020). They were sequenced and then recombined into the GATEWAY binary destination vector pPURO-Flag-HA (gift from Dr. Sebastien Pfeffer, IBMC, Strasbourg, France) using LR clonase (Invitrogen, 11791020), hereinafter referred to as pFlag, allowing an expression under the control of the cytomegalovirus (CMV) immediate early promoter. The molecular characterization of LegK1 was then done in the HEK293T cell line, using a pPURO-2xFlag-HA, hereinafter referred to as p2xFlag. This plasmid was constructed from pFlag expression vector, by insertion of a second Flag using Gibson assembly (New England BioLabs, E5510S). The *legK1* coding sequence was then inserted from

pENTR/D-TOPO-LegK1 into p2xFlag through the GATEWAY technology, as previously described. Point mutations were introduced in this plasmid to generate the kinase-dead mutant (LegK1-KA), the mutants on the three putative W-motifs (LegK1-3WF), on the two functional W-motifs (LegK1-W283F-W293A) or on the individual W-motifs (LegK1-W283F, -W293F, -W293A). All these point mutations were carried out using site-directed mutagenesis by PCR with appropriate primers containing the desired nucleotide changes (Table S1), and followed by selection with DpnI digestion. For siRNA-guided *GFP* silencing reporter, the plasmid pPURO-Flag-HA-eGFP was cloned in this study using GATEWAY technology, as previously described, and was hereinafter referred to as pFlag-eGFP. The miRNA-guided *GFP* silencing reporter, referred to as AutomiG, was kindly provided by Pr. Christophe Antoniewski[76] (Institut de Biologie Paris Seine, Paris, France). A vector expressing TNRC6B-derived peptide (T6B) was used as positive control of the siRNA-guided GFP silencing reporter, and was kindly provided by Pr. Gunter Meister[75] (Universität Regensburg, Regensburg, Germany).

For the co-immunoprecipitation assays, a plasmid expressing human Ago2 fused to GFP in the N-terminal region of Ago2 was obtained from Addgene (11590). For recombinant protein purification, a DNA fragment encoding LegK1 amino acids 2 to 386 was amplified by PCR, digested with NotI and XhoI enzymes and inserted into pET22-His_6-SUMO plasmid[107], kindly given by Dr. Hervé Le Hir (IBENS, Paris, France). This construct allows the expression of LegK1$^{2–386}$ recombinant protein in fusion with an amino-terminal SUMO tag and a polyhistidine tag. The pET22-His_6-SUMO-LegK1$^{2-386}$-KA and pET22-His_6-SUMO-LegK1$^{2-386}$-3WF were generated using site-directed mutagenesis by PCR. The full-length GST-Ago2 was purified from the

pGST-Ago2 plasmid, obtained from Addgene (24317). A construct including only the PIWI domain of Ago2 and a fraction of MID domain was generated by PCR amplification of Ago2 amino-acids 517 to 659. PIWI$^{517-859}$ DNA was digested by BamHI and HindIII enzymes and cloned into pET28-CBP-His$_6$, kindly given by Dr. Hervé Le Hir, allowing a fusion with the Calmodulin Binding Protein (CBP) and a polyhistidine tag in amino-terminal and in carboxyl-terminal ends, respectively. Finally, the full-length IκBα was purified from pET28-CBP-IκBα-His$_6$ plasmid. IκBα DNA was PCR amplified from pBABE-GFP-IκBα-wt (Addgene, 15263) and was digested and cloned into pET28-CBP-His$_6$, as described for pET28-CBP-PIWI$^{517-859}$-His$_6$. The negative control protein TAP, consisting of the CBP and His$_6$ tags, was purified from a plasmid pET28 derivative, kindly provided by Dr. Hervé Le Hir[107]. For complementation assay, the full-length *legK1* gene was cloned under the control of its own promoter into pBC-KS (Stratagene, 212215) using SacI and KpnI restriction enzymes. All constructions were confirmed by Sanger sequencing.

Human cell transfections

For the detection of recombinant LegK1 WT or mutant proteins by Western blot analysis, HEK293T cells were seeded in 24-well plates at a density of 1.4x10^5 cells per well, and were transiently transfected for 48h with either 500 ng of p2xFlag-LegK1-WT, -KA or -3WF plasmids using JetPrime (Polyplus, 114-15), according to the manufacturer's instructions.

For the characterization of the siRNA-based luciferase reporter, control (CTL), *ago1*$^{-/-}$, *ago2*$^{-/-}$, *ago1*$^{-/-}$/*ago2*$^{-/-}$ and *dicer*$^{-/-}$ HeLa cell lines were transfected with Lipofectamine 2000 (Invitrogen, 11668019). One day before transfection, HeLa cell lines were

trypsinized, resuspended in DMEM, and seeded in 48-well plates at a density of $7x10^4$ cells per well. Cells were transiently co-transfected for 48h with 100 ng of pGL3-CXCR4-2p, 50 ng of pRL-TK as transfection control, and 250 pM of AllStars Negative Control siRNA (Qiagen, 1027280) or CXCR4 siRNA (GUUUUCACUCCAGCUAACACA, Eurofins Genomics). For the initial screening of bacterial effectors, WT HeLa cells were co-transfected as previously described, with an addition of 400 ng of vector expressing a bacterial candidate or HBx as positive control. Firefly and Renilla luciferase expressions were determined as described in the Dual-luciferase silencing reporter analyses section. For the siRNA-based GFP sensor, HeLa and HEK293T cell lines were seeded in 24-well plates at the same density as mentioned above. Cells were co-transfected for 48h with 200 ng of pFlag-eGFP and 30 pmol of GFP RNA duplex (RNA GFP duplex I, Thermoscientific, P-002048-01-20) or AllStars Negative Control siRNA, and with 1 μg of p2xFlag-LegK1-WT, -KA, -3WF, -W283F, -W293F, -W293A, -W283F-W293A, pFlag-YopM or empty vector as negative control, or pFlag-T6B as positive control using Lipofectamine 2000. GFP proteins levels were next analysed by Western blot. For the miRNA-based GFP sensor, HEK293T cells were seeded in 24-well plates at the same density as previously described and cells were co-transfected with 200 ng of AutomiG and 1μg of plasmid expressing either WT or LegK1 mutants, YopM or T6B using Lipofectamine 2000 for 48h. GFP protein levels were further analysed by Western blot analyses.

For the co-immunoprecipitation assays, HEK293T cells were seeded in 10 cm^2 dishes at a density of $6.2x10^6$ cells per well and were transiently transfected during 48h with 10 μg of pFlag-eGFP or p2xFlag-LegK1-WT, -KA, -3WF using JetPrime. For the co-immunoprecipitation assay followed by RNAse A treatment (Thermo Scientific,

R1253), HEK293T cells were seeded in the same manner and were co-transfected for 48h with 10 μg of pGFP-Ago2-WT and 10 μg of pFlag-T6B or 14 μg of p2xFlag-LegK1 using Lipofectamine 2000. To determine the catalytic activity of LegK1 mutants in the kinase assay, HEK293T cells were seeded in 6 cm^2 dishes at a density of $8.4x10^5$ cells per well, and were transiently transfected for 48h with 4 μg of pFlag-eGFP or p2xFlag-LegK1-WT or p2xFlag-LegK1 mutants using JetPrime. Finally, for the mass spectrometry analysis, HeLa cells were seeded in 15 cm^2 dishes at a density of $1.4x10^7$ cells per well and were transfected for 24h with 20 μg of pFlag-eGFP, p2xFlag-LegK1-WT or -KA using JetPrime.

A. castellanii and THP-1 infection assays

A. castellanii were washed once with Infection Buffer (PYG 712 medium without proteose peptone, glucose and yeast extract) and seeded in 25 cm^2 flasks at a concentration of $4x10^6$ cells per flask. *L. pneumophila* WT and mutant strains were grown on BCYE agar to stationary phase, diluted in Infection Buffer and mixed with *A. castellanii* at a Multiplicity Of Infection (MOI) of 0.1 or 1 for complementation experiments. After a 1h invasion period, the *A. castellanii* layer was washed three times with Infection Buffer. For every time point, the intracellular multiplication of bacteria was monitored collecting 300 µL of sample, that were centrifuged (14,500 rpm, 10 min) and vortexed to break up amoeba and plated on BCYE plates. For THP-1 infection, cells were seeded into 12-well tissue culture trays at a density of $2x10^5$ cells per well and pretreated with 10^{-8} M phorbol 12-myristate 13-acetate (PMA) (Sigma) for 72 h, in 5% CO_2 at 37°C, to induce differentiation into macrophage-like adherent cells. Stationary phase *Legionella* were resuspended in RPMI 1640 serum free medium and added to THP-1 cells monolayer at a MOI of 10. After a 2h incubation,

cells were washed with1X PBS before incubation with serum-free medium. At 24h, 48h and 72h post-infection, THP-1 cells were lysed with 0.1% Triton X-100. The *Legionella* titers were monitored by counting the number of colony-forming units (CFU) after plating on BCYE agar.

Dual-luciferase silencing reporter analyses

The initial screening in HeLa cells was carried out using a siRNA-guided luciferase silencing reporter, consisting in the expression of the pGL3-CXCR4-2p vector[71], along with CXCR4 RNA duplexes. In parallel, a Renilla luciferase control reporter vector was used, corresponding to the pRL-TK. Transfected cells were washed with 1X PBS and then lysed in 65 μL of 1X Passive Lysis Buffer (Dual-Luciferase Reporter Assay System, Promega, E1910) by shaking for 15 min at room temperature. Firefly and Renilla activities were measured in 10 μL of cell lysate with the Luciferase reporter assay system, according to the supplier's protocol. Briefly, bioluminescence was initiated by automatic injection of 30 μL of Luciferase Assay Reagent II. After a 1-second shaking and an additional 1-second delay, Firefly luciferase emission signals were recorded on TriStar LB 941 Multimode Microplate Reader luminometer (Berthold Technologies), using a 10-second measurement period for each condition. The Renilla luciferase emission signals were then measured after injection of 30 μL of Stop & Glo Reagent, in the same manner as for Firefly luminescence detection. All measurements were carried out in three technical replicates for each independent experiment. Firefly luminescence expression was corrected with the Renilla control, the luminescence value of siCXCR4 condition was then normalised on siCTL condition, and further normalised by the negative control condition, corresponding to the CTL HeLa cell line or eGFP transfected WT HeLa cells.

GFP-based silencing reporter system analyses

The suppression activities on siRNA- and miRNA-guided *GFP* silencing reporters were both determined by Western blot analyses. Transfected cells were washed with 1X PBS and lysed in 100 μL of 1X Laemmli Loading Buffer. For each condition, 40 μL of samples were loaded on SDS-PAGE and subjected to Western Blot analysis. In some experiments, cells were transiently co-transfected with siRNA-guided silencing reporters and p2xFlag-LegK1 or pFlag empty control plasmid or pFlag-YopM, to ensure that each transfection received the same amount of total DNA. For the inhibition of NF-κB signaling, cells were then treated for 1h with 25 μg/mL of Caffeic Acid Phenethyl Ester inhibitor (CAPE, Santa Cruz Biotechnology, sc-200800) or DMSO. Cell extracts were subjected to Western blot analysis, as described previously. Quantification of eGFP protein from Western blot analysis was performed by densitometric analysis, using the Fiji (ImageJ) software, and was then normalised to the YopM-siCTL or empty vector-siCTL conditions.

Western blot analyses

Cells were washed with 1X PBS and lysed either in 1X Laemmli Loading Buffer or in Radio-ImmunoPrecipitation Assay (RIPA) buffer, for which the protein concentration was determined using the Bradford reagent (Bio-Rad, 5000006EDU). Approximately 100 μg of proteins were denatured 5 min at 95°C and then subjected to SDS-PAGE and Western blot analyses, according to standard procedures. The detection of proteins of interest was performed using the following primary antibodies: anti-Ago1 (D84G10, Cell Signaling Technology, 5053), anti-Ago2 (C34C6, Cell Signaling Technology, 2897), anti-Ago3 (4B1-F6, Active Motif, 39787), anti-Ago4 (D10F10, Cell Signaling Technology, 6913), anti-DDX6 (Bethyl, A300-460A), anti-Dicer (Cell

Signaling Technology, 3363), anti-Flag (M2, Sigma-Aldrich, F1804), anti-GAPDH (14C10, Cell Signaling Technology, 2118), anti-GFP (D5.1, Cell Signaling Technology, 2956), anti-PABPC1 (Atlas Antibodies, HPA045423), anti-phospho-IκBα (Ser32) (14D4, Cell Signaling Technology, 2859), anti-TNRC6A (Bethyl, A302-329A) and anti-α-Tubulin (DM1A, Cell Signaling Technology, 3873). Both antibodies were diluted 1000×. As secondary antibodies, anti-mouse (Cell Signaling Technology, 7076S) or anti-rabbit (Cell Signaling Technology, 7074S) were used and proteins were detected with Agrisera ECL SuperBright (Agrisera, AS16 ECL-S-100) using a LAS 4000 mini (GE Healthcare).

Co-immunoprecipitation analyses

Cells were transiently transfected in 10 cm^2 dishes, harvested at 48h post-transfection, washed twice with ice cold 1X PBS and lysed with Lysis Buffer (20 mM, Tris–HCl [pH 7.4], 150 mM NaCl, 2 mM EDTA, 0.5% NP-40, 1 mM DTT, 1X protease inhibitor [EDTA-free complete Protease Inhibitor Cocktail, Roche, 11873580001] and 1:100 phosphatase inhibitor [Sigma-Aldrich, P5726]). In some experiments, cell lysates were treated with 100 ng/μL of RNase A (ThermoFisher, R1253) for 1h at 37°C. The RNAse A treatment was checked on agarose gel by loading some input extract (data not shown). For each condition, 30 µL of input were collected and the concentration was measured using the Bradford reagent in order to load 100 µg of input proteins for the following analysis. Thirty µl of Dynabeads Protein G (Invitrogen, 10003D) were incubated with 7 μg of anti-FLAG M2 antibody (Sigma-Aldrich, F1804) for 1h30 at 4°C in 1X PBS containing 0.1% of Tween20. Dynabeads Protein G linked to the antibodies were then incubated overnight with cell lysates at 4°C under agitation. The immunoprecipitates were washed three times with IP Buffer (50 mM Tris–HCl (pH 7.4),

from 150 mM to 250 mM NaCl, 0.05% NP-40, 1X protease inhibitor and phosphatase inhibitor) and eluted in 4X Laemmli Loading Buffer. Protein samples were denatured 5 min at 95°C, resolved on SDS-PAGE gel and analysed by Western blot.

Purification of recombinant proteins

All recombinant proteins were expressed from the *E. coli* strain BL21(DE3) codon plus (ThermoFisher, EC0114) in 1L of Terrific broth (TB). Cultures were grown at 37°C until they reached an OD_{600} of 2 and protein production was induced with 1 mM Isopropyl-β-D-thiogalactopyranoside (IPTG), followed by overnight growth at 18°C with shaking at 180 rpm. Bacterial cells expressing His_6-SUMO-LegK1$^{2–386}$, His_6-SUMO-LegK1-KA$^{2–386}$, CBP-PIWI$^{517-859}$-His_6, CBP-IκBα-His_6 and His_6-TAP were collected by centrifugation, resuspended in Lysis Buffer (1.5X PBS, 1 mM $MgAc_2$, 0,1 % NP-40, 20 mM imidazole, 10 % glycerol), and lysed by sonication during 4 min on ice. Lysate was clarified by high-speed centrifugation (18,000 rpm) and then purified on 250 μL of Ni-NTA resin (Thermo Fisher Scientific, 88221). Resin was pre-equilibrated in Lysis Buffer, and supernatant was incubated with resin for 2h at 4°C. His fusion proteins linked to the resin were washed once with Lysis Buffer, then once with Wash Buffer (1.5X PBS, 250 mM NaCl, 1 mM $MgAc_2$, 0.1 % NP-40, 50 mM imidazole, 10 % glycerol), and finally with Lysis Buffer. Proteins were eluted in Elution Buffer (1.5X PBS, 1 mM $MgAc_2$, 0.1 % NP-40, 150 mM imidazole, 10 % glycerol). Excess imidazole was removed by overnight dialysis using Spectrum™ Labs Spectra/Por™ 2 12-14 kD MWCO (FisherScientific, 15310762) into Dialysis Buffer (1.5X PBS, 1 mM $MgAc_2$, 10 % glycerol, 2 mM DTT) before storage at -80°C.

Bacterial cells expressing GST-Ago2 recombinant protein were collected by centrifugation, resuspended in Lysis Buffer (1.5X PBS, 1 mM $MgAc_2$, 1mM DTT, 0.1% NP-40, 10% glycerol), and lysed by sonication during 4 min on ice. Lysate was clarified by high-speed centrifugation and then purified on 500 μL of Glutathione Sepharose 4B resin (Merck, GE-17-0756-01). Beads were pre-equilibrated in Lysis Buffer and supernatant was incubated with resin for 2h at 4°C. GST fusion proteins linked to the beads were washed once with Lysis Buffer, then once with Wash Buffer (1.5X PBS, 250 mM KCl, 1 mM $MgAc_2$, 1 mM DTT, 0.1 % NP-40, 10 % glycerol), and finally with Lysis Buffer. Proteins were eluted in Elution Buffer (50 mM Tris pH8.0, 250 mM KCl, 1 mM $MgAc_2$, 1 mM DTT, 0.1 % NP-40, 10 % glycerol, 10 mM reduced glutathione). Proteins were subjected to overnight dialysis using the same dialysis tubing as mentioned above into Dialysis Buffer (10 mM HEPES pH7.5, 250 mM KCl, 1 mM $MgAc_2$, 10 % glycerol, 2 mM DTT) before storage at -80°C. All recombinant protein concentrations were determined using the Bradford reagent. Proteins were analysed by Coomassie Blue staining after SDS-PAGE.

***In vitro* interaction assays**

Glutathione Sepharose 4B resin and Calmodulin Affinity Resin (Agilent Technologies, 214303) were washed twice with Blocking Buffer (20 mM Hepes pH 7.5, 150 mM NaCl, 0.1 % NP-40) and then blocked into Blocking Buffer supplemented with 20 mM NaCl, 2 mg/mL glycogen carrier, 10 mg/mL tRNA and 10 mg/mL BSA during 2h at 4°C. Subsequently, beads were washed twice with Blocking Buffer and resuspended into Storage Buffer (10 mM HEPES pH 7.5, 250 mM NaCl, 1 mM EDTA). For *in vitro* interaction assays using GST pull-down, 5 μg of each purified protein were incubated in B1.5 Buffer (1.5X PBS, 1 mM $MgAc_2$, 2 mM DTT, 10% glycerol). The same volume

of 2X BB Buffer (40 mM Hepes pH 7.5, 83 mM NaCl, 1 mM $MgAc_2$, 0.2% NP-40, 11.7% glycerol, 2 mM DTT) was added. After 20 min of interaction at 30°C under rotation, 12 µL of Glutathione Sepharose 4B were added. Beads were washed three times with 500 µL of 1X BB 250/10 Buffer (20 mM HEPES pH 7.5, 250 mM NaCl, 1 mM $MgAc_2$, 0,2 % NP-40, 10 % glycerol, 1 mM DTT), and then proteins were eluted by incubation with 20 µL of Elution Buffer (50 mM Tris·HCl (pH 7.5), 250 mM KCl, 1 mM $MgAc_2$, 1 mM DTT, 0.1 % NP-40, 10 % glycerol, 10 mM reduced Glutathione) for 5 min at 30 °C, under shaking at 1,400 rpm. Finally, proteins bound to GST beads were eluted with Elution Buffer for 5 min at 30 °C, under shaking at 1,400 rpm. 4X Laemmli Loading Buffer was added and proteins were separated onto SDS-PAGE gel and analysed by Western blot.

For binding assays using CBP pull-down, proteins were prepared according to the same protocol as mentioned above. In some experiments, from 5 to 15 µg of human cell extracted RNAs were incubated with protein samples. After 20 min of interaction at 30°C under rotation, 12 µL of Calmodulin Affinity Resin were added. Beads were washed three times with 500 µL of 1X BB 250/10 Buffer (20 mM Hepes pH=7.5, 250 mM NaCl, 2 mM $MgAc_2$, 2 mM imidazole, 2 mM $CaCl_2$, 0.1 % NP-40, 10 % glycerol, 1 mM DTT). Proteins were eluted by incubation with 20 µL of Elution Buffer (10 mM Tris·HCl (pH 7.5), 250 mM KCl, 1 mM $MgAc_2$, 1 mM DTT, 0.1 % NP-40, 10 % glycerol, 20 mM EGTA) for 5 min at 30 °C, under shaking at 1,400 rpm. 4X Laemmli Loading Buffer was added and proteins were separated onto SDS/PAGE gel and analysed by Western blot.

Kinase assays

In vitro phosphorylation of 1 μg of purified GST-Ago2 or CBP-IκBα-His_6 recombinant proteins was performed in the presence of 1 μg of His_6-SUMO-LegK1$^{2–386}$ or His_6-SUMO-LegK1$^{2–386}$-KA in 20 μl of phosphorylation buffer, containing 25 mM Tris HCl (pH 7.5), 200 mM NaCl, 10 mM $MgCl_2$, and 50 μM unlabeled ATP. Reactions were split in two, and in one half 10 μCi [γ-32P] ATP were added. The phosphorylation reaction was performed for 1h at 30°C and stopped by adding 4X Laemmli Loading Buffer. A Western blot analysis was carried out on unlabeled samples. Labeled samples were analysed by SDS-PAGE, which was exposed to a phosphor screen and visualised by Typhoon FLA 9500 biomolecular imager.

The kinase activity of LegK1 mutant versions was determined using IκBα recombinant protein. For this, HEK293T cells were seeded in 6 cm^2 dishes and transfected with either pFlag-eGFP, p2xFlag-LegK1-WT, -KA, -3WF, -W283F, -W293F, -W293A or -W283F-W293A. Cells were lysed and subjected to a Flag immunoprecipitation. The resulting immunoprecipitates were incubated with Phosphorylation Buffer (250 mM Tris-HCl pH 7.5, 50 mM $MnCl_2$, 50 mM DTT) and 1 μg of purified CBP-IκBα-His_6 recombinant proteins for 30 min at 30°C. Proteins were mixed with 4X Laemmli Loading Buffer and then analysed by Western blot using the phospho-IκBα (Ser32) (14D4) antibody.

Peptide pull-down assays

Biotinylated peptides (synthetised by Genscript) were resuspended in DMSO, and heated at 40°C for 5 min. For binding assays, 10 μg of peptides were diluted into 200 μL of PBS containing 0.1% of Tween20, and were incubated for 30 min at room

temperature in the presence of 30 µL of Dynabeads MyOne™ Streptavidin T1 (Thermo Fisher Scientific, 65601). The beads were then washed once in 0.1% PBS Tween and twice in IP Buffer (50 mM Tris-HCl pH 7.4, 150 mM NaCl, 5 mM $MgCl_2$, 0.05% NP-40, 1/100 Phosphatase inhibitor and 1X protease inhibitor). HEK293T cells were washed twice with ice cold 1X PBS and scraped with Lysis Buffer (see the Co-immunoprecipitation analyses section). Some cell lysate were collected and the concentration was measured using the Bradford reagent in order to load 80 µg of input proteins for the following analysis. Cells were incubated at 4°C under rotation for 30 min and the supernatant was harvested by centrifugation at 16,000 g for 10 min at 4°C. Beads-coupled peptides were incubated in the presence of cell lysates for 1 hour at 4°C After three washing steps of the beads with IP Buffer, the proteins were eluted in 4X Laemmli Loading Buffer and resolved on SDS-PAGE. The presence of Ago proteins was detected by Western blot analyses.

RNA extractions and RT-qPCR

For gene expression analyses, total RNAs were isolated by phenol-chloroform extraction using TRIzol Reagent (Thermo Fisher Scientific, 15-596-018), according to the manufacturer's instructions. Approximately 0.5 µg of RNAs were then digested by DNAse I (Promega, M6101) at 37°C for 50 min to remove the genomic DNA, followed by 10 min at 65°C to inactivate the DNAse. DNAse-digested RNAs were reverse-transcribed into complementary DNA using qScript cDNA Supermix (Quanta Biosciences, 733-1178). The cDNAs were quantified with SYBR Green qPCR mix (Takyon, Eurogentec, UF-NSMT-B0701) and gene-specific primers (Table S1) in 384-well plates, following a protocol of heating at 95°C for 10 min, 45 cycles of denaturation at 95°C for 10 sec, and annealing at 60°C for 40 sec. A melting curve was performed

at the end of the amplification, and transcript levels were then normalised to the abundance of *GAPDH* transcripts.

PRM data acquisition method

HeLa cells were seeded in 15 cm^2 dishes at a density of $1.4x10^7$ cells, and transiently transfected with either pFlag-eGFP, p2xFlag-LegK1-WT or -KA. At 24h post-transfection, cells were washed twice with ice cold 1X PBS and lysed with Lysis Buffer (see the Co-immunoprecipitation analyses section). For each condition, 30 µL of input were collected and analysed by Western blot. Sixty µl of Dynabeads Protein G were incubated for 1h30 at 4°C under agitation with 16 µg of the anti-Ago2 antibody (Sigma-Aldrich, SAB4200085) in 1X PBS containing 0.1% of Tween 20. Dynabeads Protein G linked to Ago2 antibody were then incubated overnight with cell lysates at 4°C under agitation. The immunoprecipitates were washed three times with IP Buffer (see the Co-immunoprecipitation analyses section) and eluted in 4X Laemmli Loading Buffer. Five immunoprecipitations of each condition were performed. Protein samples were denatured 5 min at 95°C, then were simultaneously separated on SDS-PAGE and stained with colloidal blue (LabSafe Gel Blue, Gbiosciences, 786-35). One gel slice was excised for each purification and in-gel digested by using trypsin/LysC (Promega, V5072). Peptides extracted from each band were then loaded onto a homemade C18 StageTips for desalting. Peptides were eluted using 40/60 MeCN/H_2O + 0.1 % formic acid and vacuum concentrated to dryness. Peptide samples were resuspended in Buffer A (2/98 MeCN/H_2O in 0.1 % formic acid), separated and analysed by nanoLC-MS/MS using an RSLCnano system (Thermo Scientific, Ultimate 3000) coupled online to a Q Exactive HF-X mass spectrometer (Thermo Scientific). Peptides were first trapped onto a C18 column (75 µm inner diameter × 2 cm; nanoViper Acclaim

PepMapTM 100, Thermo Scientific) with Buffer A at a flow rate of 2.5 µL/min over 4 min. Separation was performed on a 50 cm x 75 µm C18 column (Thermo Scientific, nanoViper C18, 3 µm, 100Å, Acclaim PepMapTM RSLC) regulated to 50°C and with a linear gradient from 2% to 30% of buffer B (100% MeCN in 0.1% formic acid) at a flow rate of 300 nL/min over 91 min. The mass spectrometer was operated in Parallel Reaction Monitoring (PRM) mode (see acquisition list Table S2). The acquisition list was generated from the peptides obtained from the mix samples (5 replicates) of each condition, based on the data-dependent acquisition (DDA) results (data not shown).

PRM data analyses

The PRM data were analysed using Skyline 4.1 (MacCoss Lab Software, Seattle, Washington [https://skyline.ms/project/home/software/Skyline/begin.view]). Fragment ions for each targeted mass (Table S3) were extracted and peak areas were integrated. The peptide areas were log2 transformed and the mean log2- area was normalised by the mean area of five Ago2 peptides (ELLIQFYK, SGNIPAGTTVDTK, SIEEQQKPLTDSQR, VELEVTLPGEGK and VLQPPSILYGGR) using software R 3.1.0. On each phospho-peptide, a linear model was used to estimate the mean fold change between the conditions, its 95% confidence interval and the p-value of the two-sided associated t-test. The p-values were adjusted with the Benjamini-Hochberg procedure[108]. Data are available via ProteomeXchange with identifier PXD037279 (Username: reviewer_pxd037279@ebi.ac.uk; Password: xzomxsb6)[109].

Prediction of W-motifs

W-motifs were predicted using the Wsearch algorithm[70], which scores the W-motifs according to a Position-Specific Scoring Matrice (PSSM) derived from experimentally

validated Ago-binding motifs from animals. Briefly, the protein sequences of all bacterial organisms tested were retrieved from Uniprot (UniProt Consortium, 2018) and subjected to Wsearch either on the website or using the python script. The score of the different positive motifs were then added together, corresponding to the final score. For the first pre-selection, we applied an arbitrary cut-off greater than six on the average W-scores of all motifs present in the candidate protein sequence. Among the bacterial candidate proteins exhibiting the highest W-score, we further selected known secreted virulence factors or putative virulence factors predicted to be secreted using PSORTb 3.0 (https://www.psort.org/psortb/)[110].

Alignment of orthologous protein sequences and phylogeny

The protein sequence of LegK1 (from the *lpp1439* gene) from *L. pneumophila* strain Paris was used as a reference to retrieve homologous LegK1 protein sequences from *Legionella* species (taxid: 445). To this end, a BLASTP (Basic Local Alignment Search Tool) was performed on the NCBI (National Center for Biotechnology Information) website. An identity cut-off of 40%, an Expect (E)-value cut-off of 10^{-5} and a minimum percentage match length of subject and query of 65% were used. The set of homologous protein sequences were then aligned using ClustalW2 on Geneious 10.2.6 software. Tree was conducted using Neighbor-joining.

Heatmap of *Ago* transcripts

The RNA-sequencing results were generated in the Cancer Cell Line Encyclopedia (CCLE, Primary ID: E-MTAB-2770) and are reported as linear values, retrieved from Genevestigator.

Quantification and statistical analysis

Experimental results were shown as standard error of the mean (SEM) for luciferase reporter and qPCR experiments and as standard deviation (SD) for infection assays. Statistical analysis was carried out using the Prism Software (GraphPad Prism 9.0). For statistical comparison between two groups or several conditions, an unpaired t test or one-way analysis of variance (ANOVA) of biological replicates were used, respectively. For infection assays, a Wilcoxon test was used. A value of $P < 0.05$ was considered statistically significant. All statistical tests are specified in the respective figure legends.

Data availability

All materials generated in this study are available upon request. Mass spectrometry data are available *via* ProteomeXchange with identifier PXD037279. Sequencing data corresponding to the mutant *ΔlegK1* have been submitted to Zenodo (https://zenodo.org/record/7190772). All data reported in this paper will be shared by the lead contact upon request.

Correspondence and requests for materials should be addressed to Lionel Navarro (lionel.navarro@ens.psl.eu).

References

1. Rowbotham, T. J. Preliminary report on the pathogenicity of *Legionella pneumophila* for freshwater and soil amoebae. *J Clin Pathol* **33**, 1179–1183 (1980).

2. Newton, H. J., Ang, D. K. Y., van Driel, I. R. & Hartland, E. L. Molecular pathogenesis of infections caused by *Legionella pneumophila*. *Clin Microbiol Rev* **23**, 274–298 (2010).

3. Boamah, D. K., Zhou, G., Ensminger, A. W. & O'Connor, T. J. From Many Hosts, One Accidental Pathogen: The Diverse Protozoan Hosts of *Legionella*. *Front Cell Infect Microbiol* **7**, 477 (2017).

4. Mondino, S. *et al.* Legionnaires' Disease: State of the Art Knowledge of Pathogenesis Mechanisms of *Legionella*. *Annual Review of Pathology: Mechanisms of Disease* **15**, 439–466 (2020).

5. Escoll, P., Rolando, M., Gomez-Valero, L. & Buchrieser, C. From Amoeba to Macrophages: Exploring the Molecular Mechanisms of *Legionella pneumophila* Infection in Both Hosts. in *Molecular Mechanisms in Legionella Pathogenesis* (ed. Hilbi, H.) 1–34 (Springer, 2014). doi:10.1007/82_2013_351.

6. Marra, A., Blander, S. J., Horwitz, M. A. & Shuman, H. A. Identification of a *Legionella pneumophila* locus required for intracellular multiplication in human macrophages. *Proc Natl Acad Sci U S A* **89**, 9607–9611 (1992).

7. Berger, K. H. & Isberg, R. R. Two distinct defects in intracellular growth complemented by a single genetic locus in *Legionella pneumophila*. *Mol Microbiol* **7**, 7–19 (1993).

8. Segal, G., Purcell, M. & Shuman, H. A. Host cell killing and bacterial conjugation require overlapping sets of genes within a 22-kb region of the *Legionella pneumophila* genome. *Proc Natl Acad Sci U S A* **95**, 1669–1674 (1998).

9. Burstein, D. *et al.* Genome-Scale Identification of *Legionella pneumophila* Effectors Using a Machine Learning Approach. *PLOS Pathogens* **5**, e1000508 (2009).

10. Huang, L. *et al.* The E Block motif is associated with *Legionella pneumophila* translocated substrates. *Cell Microbiol* **13**, 227–245 (2011).

11. Zhu, W. *et al.* Comprehensive Identification of Protein Substrates of the Dot/Icm Type IV Transporter of *Legionella pneumophila*. *PLOS ONE* **6**, e17638 (2011).

12. Lifshitz, Z. *et al.* Computational modeling and experimental validation of the *Legionella* and *Coxiella* virulence-related type-IVB secretion signal. *Proc Natl Acad Sci U S A* **110**, E707-715 (2013).

13. Gomez-Valero, L. *et al.* More than 18,000 effectors in the *Legionella* genus genome provide multiple, independent combinations for replication in human cells. *Proc Natl Acad Sci U S A* **116**, 2265–2273 (2019).

14. Cazalet, C. *et al.* Evidence in the *Legionella pneumophila* genome for exploitation of host cell functions and high genome plasticity. *Nat Genet* **36**, 1165–1173 (2004).

15. de Felipe, K. S. *et al.* Evidence for Acquisition of *Legionella* Type IV Secretion Substrates via Interdomain Horizontal Gene Transfer. *J Bacteriol* **187**, 7716–7726 (2005).

16. Lurie-Weinberger, M. N. *et al.* The origins of eukaryotic-like proteins in *Legionella pneumophila. Int J Med Microbiol* **300**, 470–481 (2010).

17. Ge, J. *et al.* A *Legionella* type IV effector activates the NF-κB pathway by phosphorylating the IκB family of inhibitors. *Proc Natl Acad Sci U S A* **106**, 13725–13730 (2009).

18. Losick, V. P. & Isberg, R. R. NF-kappaB translocation prevents host cell death after low-dose challenge by *Legionella pneumophila*. *J Exp Med* **203**, 2177–2189 (2006).

19. Abu-Zant, A. *et al.* Anti-apoptotic signalling by the Dot/Icm secretion system of *L. pneumophila*. *Cell Microbiol* **9**, 246–264 (2007).

20. Bartfeld, S. *et al.* Temporal resolution of two-tracked NF-κB activation by *Legionella pneumophila*. *Cellular Microbiology* **11**, 1638–1651 (2009).

21. Bartel, D. P. Metazoan MicroRNAs. *Cell* **173**, 20–51 (2018).

22. Duchaine, T. F. & Fabian, M. R. Mechanistic Insights into MicroRNA-Mediated Gene Silencing. *Cold Spring Harb Perspect Biol* **11**, a032771 (2019).

23. Iwakawa, H.-O. & Tomari, Y. Life of RISC: Formation, action, and degradation of RNA-induced silencing complex. *Mol Cell* **82**, 30–43 (2022).

24. Jonas, S. & Izaurralde, E. Towards a molecular understanding of microRNA-mediated gene silencing. *Nat. Rev. Genet.* **16**, 421–433 (2015).

25. Sasaki, T., Shiohama, A., Minoshima, S. & Shimizu, N. Identification of eight members of the Argonaute family in the human genome. *Genomics* **82**, 323–330 (2003).

26. Müller, M., Fazi, F. & Ciaudo, C. Argonaute Proteins: From Structure to Function in Development and Pathological Cell Fate Determination. *Frontiers in Cell and Developmental Biology* **7**, (2020).

27. Liu, J. *et al.* Argonaute2 Is the Catalytic Engine of Mammalian RNAi. *Science* **305**, 1437–1441 (2004).

28. Meister, G. *et al.* Human Argonaute2 mediates RNA cleavage targeted by miRNAs and siRNAs. *Mol. Cell* **15**, 185–197 (2004).

29. Schirle, N. T. & MacRae, I. J. The Crystal Structure of Human Argonaute2. *Science* **336**, 1037–1040 (2012).

30. Sheu-Gruttadauria, J. & MacRae, I. J. Phase transitions in the assembly and function of human miRISC. *Cell* **173**, 946-957.e16 (2018).

31. Li, X., Wang, X., Cheng, Z. & Zhu, Q. AGO2 and its partners: a silencing complex, a chromatin modulator, and new features. *Crit Rev Biochem Mol Biol* **55**, 33–53 (2020).

32. Till, S. *et al.* A conserved motif in Argonaute-interacting proteins mediates functional interactions through the Argonaute PIWI domain. *Nature Structural & Molecular Biology* **14**, 897–903 (2007).

33. Horman, S. R. *et al.* Akt-mediated phosphorylation of Argonaute 2 down-regulates cleavage and up-regulates translational repression of microRNA targets. *Mol Cell* **50**, 356–367 (2013).

34. Bridge, K. S. *et al.* Argonaute Utilization for miRNA Silencing Is Determined by Phosphorylation-Dependent Recruitment of LIM-Domain-Containing Proteins. *Cell Reports* **20**, 173–187 (2017).

35. Chen, Y. *et al.* A DDX6-CNOT1 complex and W-binding pockets in CNOT9 reveal direct links between miRNA target recognition and silencing. *Mol. Cell* **54**, 737–750 (2014).

36. Rouya, C. *et al.* Human DDX6 effects miRNA-mediated gene silencing via direct binding to CNOT1. *RNA* **20**, 1398–1409 (2014).

37. Braun, J. E., Huntzinger, E., Fauser, M. & Izaurralde, E. GW182 proteins directly recruit cytoplasmic deadenylase complexes to miRNA targets. *Mol. Cell* **44**, 120–133 (2011).

38. Chekulaeva, M. *et al.* miRNA repression involves GW182-mediated recruitment of CCR4-NOT through conserved W-containing motifs. *Nat. Struct. Mol. Biol.* **18**, 1218–1226 (2011).

39. Fabian, M. R. *et al.* miRNA-mediated deadenylation is orchestrated by GW182 through two conserved motifs that interact with CCR4-NOT. *Nat. Struct. Mol. Biol.* **18**, 1211–1217 (2011).

40. Christie, M., Boland, A., Huntzinger, E., Weichenrieder, O. & Izaurralde, E. Structure of the PAN3 pseudokinase reveals the basis for interactions with the PAN2 deadenylase and the GW182 proteins. *Mol Cell* **51**, 360–373 (2013).

41. Alisch, R. S., Jin, P., Epstein, M., Caspary, T. & Warren, S. T. Argonaute2 is essential for mammalian gastrulation and proper mesoderm formation. *PLoS Genet* **3**, e227 (2007).

42. Morita, S. *et al.* One Argonaute family member, Eif2c2 (Ago2), is essential for development and appears not to be involved in DNA methylation. *Genomics* **89**, 687–696 (2007).

43. Li, Y. *et al.* Induction and suppression of antiviral RNA interference by influenza A virus in mammalian cells. *Nat Microbiol* **2**, 16250 (2016).

44. Qiu, Y. *et al.* Human Virus-Derived Small RNAs Can Confer Antiviral Immunity in Mammals. *Immunity* **46**, 992-1004.e5 (2017).

45. Ngondo, R. P. *et al.* Argonaute 2 Is Required for Extra-embryonic Endoderm Differentiation of Mouse Embryonic Stem Cells. *Stem Cell Reports* **10**, 461–476 (2018).

46. Lessel, D. *et al.* Germline AGO2 mutations impair RNA interference and human neurological development. *Nat Commun* **11**, 5797 (2020).

47. Hauptmann, J. *et al.* Turning catalytically inactive human Argonaute proteins into active slicer enzymes. *Nature Structural & Molecular Biology* **20**, 814–817 (2013).

48. Park, M. S., Sim, G., Kehling, A. C. & Nakanishi, K. Human Argonaute2 and Argonaute3 are catalytically activated by different lengths of guide RNA. *PNAS* **117**, 28576–28578 (2020).

49. Nakanishi, K. Anatomy of four human Argonaute proteins. *Nucleic Acids Res* gkac519 (2022) doi:10.1093/nar/gkac519.

50. Tokita, M. J. *et al.* Five children with deletions of 1p34.3 encompassing AGO1 and AGO3. *Eur J Hum Genet* **23**, 761–765 (2015).

51. Sakaguchi, A. *et al.* Further evidence of a causal association between AGO1, a critical regulator of microRNA formation, and intellectual disability/autism spectrum disorder. *Eur J Med Genet* **62**, 103537 (2019).

52. Modzelewski, A. J., Holmes, R. J., Hilz, S., Grimson, A. & Cohen, P. E. AGO4 Regulates Entry into Meiosis and Influences Silencing of Sex Chromosomes in the Male Mouse Germline. *Developmental Cell* **23**, 251–264 (2012).

53. Miyazaki, Y., Du, X., Muramatsu, S. & Gomez, C. M. An miRNA-mediated therapy for SCA6 blocks IRES-driven translation of the CACNA1A second cistron. *Sci Transl Med* **8**, 347ra94 (2016).

54. Cheray, M. *et al.* Cytosine methylation of mature microRNAs inhibits their functions and is associated with poor prognosis in glioblastoma multiforme. *Mol Cancer* **19**, 36 (2020).

55. Chalertpet, K. *et al.* Argonaute 4 as an Effector Protein in RNA-Directed DNA Methylation in Human Cells. *Front Genet* **10**, 645 (2019).

56. Adiliaghdam, F. *et al.* A Requirement for Argonaute 4 in Mammalian Antiviral Defense. *Cell Rep* **30**, 1690-1701.e4 (2020).

57. Aguilar, C., Mano, M. & Eulalio, A. MicroRNAs at the Host–Bacteria Interface: Host Defense or Bacterial Offense. *Trends in Microbiology* **27**, 206–218 (2019).

58. Herkt, C. E. *et al.* A MicroRNA Network Controls *Legionella pneumophila* Replication in Human Macrophages via LGALS8 and MX1. *mBio* **11**, (2020).

59. Sahr, T. *et al.* Translocated *Legionella pneumophila* small RNAs mimic eukaryotic microRNAs targeting the host immune response. *Nat Commun* **13**, 762 (2022).

60. Koeppen, K. *et al.* Let-7b-5p in vesicles secreted by human airway cells reduces biofilm formation and increases antibiotic sensitivity of P. aeruginosa. *Proc Natl Acad Sci U S A* **118**, e2105370118 (2021).

61. Navarro, L., Jay, F., Nomura, K., He, S. Y. & Voinnet, O. Suppression of the microRNA pathway by bacterial effector proteins. *Science* **321**, 964–967 (2008).

62. Aqil, M., Naqvi, A. R., Bano, A. S. & Jameel, S. The HIV-1 Nef Protein Binds Argonaute-2 and Functions as a Viral Suppressor of RNA Interference. *PLoS One* **8**, (2013).

63. Li, Y., Lu, J., Han, Y., Fan, X. & Ding, S.-W. RNA Interference Functions as an Antiviral Immunity Mechanism in Mammals. *Science* **342**, (2013).

64. Maillard, P. V. *et al.* Antiviral RNA Interference in Mammalian Cells. *Science* **342**, (2013).

65. El-Shami, M. *et al.* Reiterated WG/GW motifs form functionally and evolutionarily conserved ARGONAUTE-binding platforms in RNAi-related components. *Genes Dev.* **21**, 2539–2544 (2007).

66. Azevedo, J. *et al.* Argonaute quenching and global changes in Dicer homeostasis caused by a pathogen-encoded GW repeat protein. *Genes Dev* **24**, 904–915 (2010).

67. Giner, A., Lakatos, L., García-Chapa, M., López-Moya, J. J. & Burgyán, J. Viral Protein Inhibits RISC Activity by Argonaute Binding through Conserved WG/GW Motifs. *PLoS Pathogens* **6**, e1000996 (2010).

68. Garcia, D. *et al.* Ago hook and RNA helicase motifs underpin dual roles for SDE3 in antiviral defense and silencing of nonconserved intergenic regions. *Mol Cell* **48**, 109–120 (2012).

69. Karran, R. A. & Sanfaçon, H. Tomato ringspot virus coat protein binds to ARGONAUTE 1 and suppresses the translation repression of a reporter gene. *Mol Plant Microbe Interact* **27**, 933–943 (2014).

70. Zielezinski, A. & Karlowski, W. M. Integrative data analysis indicates an intrinsic disordered domain character of Argonaute-binding motifs. *Bioinformatics* **31**, 332–339 (2015).

71. Doench, J. G., Petersen, C. P. & Sharp, P. A. siRNAs can function as miRNAs. *Genes Dev* **17**, 438–442 (2003).

72. Chinnappan, M. *et al.* Key elements of the RNAi pathway are regulated by hepatitis B virus replication and HBx acts as a viral suppressor of RNA silencing. *Biochem J* **462**, 347–358 (2014).

73. Fabozzi, G., Nabel, C. S., Dolan, M. A. & Sullivan, N. J. Ebolavirus proteins suppress the effects of small interfering RNA by direct interaction with the mammalian RNA interference pathway. *J. Virol.* **85**, 2512–2523 (2011).

74. Li, W.-X. *et al.* Interferon antagonist proteins of influenza and vaccinia viruses are suppressors of RNA silencing. *Proc. Natl. Acad. Sci. U.S.A.* **101**, 1350–1355 (2004).

75. Hauptmann, J. *et al.* Biochemical isolation of Argonaute protein complexes by Ago-APP. *Proc Natl Acad Sci U S A* **112**, 11841–11845 (2015).

76. Carré, C. *et al.* AutomiG, a Biosensor to Detect Alterations in miRNA Biogenesis and in Small RNA Silencing Guided by Perfect Target Complementarity. *PLOS ONE* **8**, e74296 (2013).

77. Fabian, M. R. *et al.* Mammalian miRNA RISC recruits CAF1 and PABP to affect PABP-dependent deadenylation. *Mol Cell* **35**, 868–880 (2009).

78. Mathys, H. *et al.* Structural and biochemical insights to the role of the CCR4-NOT complex and DDX6 ATPase in microRNA repression. *Mol. Cell* **54**, 751–765 (2014).

79. Kamenska, A. *et al.* The DDX6–4E-T interaction mediates translational repression and P-body assembly. *Nucleic Acids Research* **44**, 6318–6334 (2016).

80. Lian, S. L. *et al.* The C-terminal half of human Ago2 binds to multiple GW-rich regions of GW182 and requires GW182 to mediate silencing. *RNA* **15**, 804–813 (2009).

81. Takimoto, K., Wakiyama, M. & Yokoyama, S. Mammalian GW182 contains multiple Argonaute-binding sites and functions in microRNA-mediated translational repression. *RNA* **15**, 1078–1089 (2009).

82. Pfaff, J. *et al.* Structural features of Argonaute-GW182 protein interactions. *Proc Natl Acad Sci U S A* **110**, E3770-3779 (2013).

83. Eulalio, A., Tritschler, F. & Izaurralde, E. The GW182 protein family in animal cells: New insights into domains required for miRNA-mediated gene silencing. *RNA* **15**, 1433–1442 (2009).

84. Natarajan, K., Singh, S., Burke, T. R., Grunberger, D. & Aggarwal, B. B. Caffeic acid phenethyl ester is a potent and specific inhibitor of activation of nuclear transcription factor NF-kappa B. *Proc Natl Acad Sci U S A* **93**, 9090–9095 (1996).

85. Lee, Y. *et al.* Caffeic acid phenethyl ester-mediated Nrf2 activation and IkappaB kinase inhibition are involved in NFkappaB inhibitory effect: structural analysis for NFkappaB inhibition. *Eur J Pharmacol* **643**, 21–28 (2010).

86. Hruz, T. *et al.* Genevestigator v3: a reference expression database for the meta-analysis of transcriptomes. *Adv Bioinformatics* **2008**, 420747 (2008).

87. Karlowski, W. M. *et al.* Genome-wide computational identification of WG/GW Argonaute-binding proteins in *Arabidopsis*. *Nucleic Acids Res* **38**, 4231–4245 (2010).

88. Gomez-Valero, L. *et al.* Comparative analyses of *Legionella* species identifies genetic features of strains causing Legionnaires' disease. *Genome Biol* **15**, 505 (2014).

89. Zhang, H., Pompey, J. M. & Singh, U. RNA interference in *Entamoeba histolytica*: implications for parasite biology and gene silencing. *Future Microbiol* **6**, 103–117 (2011).

90. Matthey-Doret, C. *et al.* Chromosome-scale assemblies of *Acanthamoeba castellanii* genomes provide insights into *Legionella pneumophila* infection-related chromatin reorganization. *Genome Res* (2022) doi:10.1101/gr.276375.121.

91. Hamilton, A. J. & Baulcombe, D. C. A Species of Small Antisense RNA in Posttranscriptional Gene Silencing in Plants. *Science* **286**, 950–952 (1999).

92. Lu, R. *et al.* Animal virus replication and RNAi-mediated antiviral silencing in *C elegans*. *Nature* **436**, 1040–1043 (2005).

93. Wang, X.-H. *et al.* RNA interference directs innate immunity against viruses in adult *Drosophila*. *Science* **312**, 452–454 (2006).

94. Ding, S.-W. RNA-based antiviral immunity. *Nat Rev Immunol* **10**, 632–644 (2010).

95. Jin, Y., Zhao, J.-H. & Guo, H.-S. Recent advances in understanding plant antiviral RNAi and viral suppressors of RNAi. *Curr Opin Virol* **46**, 65–72 (2021).

96. Maillard, P. V. *et al.* Inactivation of the type I interferon pathway reveals long double-stranded RNA-mediated RNA interference in mammalian cells. *The EMBO Journal* **35**, 2505–2518 (2016).

97. van der Veen, A. G. *et al.* The RIG-I-like receptor LGP2 inhibits Dicer-dependent processing of long double-stranded RNA and blocks RNA interference in mammalian cells. *EMBO J.* **37**, (2018).

98. Xu, Y.-P. *et al.* Zika virus infection induces RNAi-mediated antiviral immunity in human neural progenitors and brain organoids. *Cell Res.* **29**, 265–273 (2019).

99. Poirier, E. Z. *et al.* An isoform of Dicer protects mammalian stem cells against multiple RNA viruses. *Science* **373**, 231–236 (2021).

100. Morel, J.-B. *et al.* Fertile Hypomorphic ARGONAUTE (ago1) Mutants Impaired in Post-Transcriptional Gene Silencing and Virus Resistance. *Plant Cell* **14**, 629–639 (2002).

101. Zhang, X. *et al.* Arabidopsis Argonaute 2 Regulates Innate Immunity via miRNA393∗-Mediated Silencing of a Golgi-Localized SNARE Gene, MEMB12. *Molecular Cell* **42**, 356–366 (2011).

102. Li, Y. *et al.* Identification of MicroRNAs Involved in Pathogen-Associated Molecular Pattern-Triggered Plant Innate Immunity. *Plant Physiology* **152**, 2222–2231 (2010).

103. Harvey, J. J. W. *et al.* An antiviral defense role of AGO2 in plants. *PLoS One* **6**, e14639 (2011).

104. Eckenfelder, A. *et al.* Argonaute proteins regulate HIV-1 multiply spliced RNA and viral production in a Dicer independent manner. *Nucleic Acids Res* **45**, 4158–4173 (2017).

105. Feeley, J. C. *et al.* Charcoal-yeast extract agar: primary isolation medium for *Legionella pneumophila*. *J Clin Microbiol* **10**, 437–441 (1979).

106. Beloin, C. *et al.* Global impact of mature biofilm lifestyle on Escherichia coli K-12 gene expression. *Mol Microbiol* **51**, 659–674 (2004).

107. Chamieh, H., Ballut, L., Bonneau, F. & Le Hir, H. NMD factors UPF2 and UPF3 bridge UPF1 to the exon junction complex and stimulate its RNA helicase activity. *Nat Struct Mol Biol* **15**, 85–93 (2008).

108. Benjamini, Y. & Yekutieli, D. The control of the false discovery rate in multiple testing under dependency. *The Annals of Statistics* **29**, 1165–1188 (2001).

109. Perez-Riverol, Y. *et al.* The PRIDE database resources in 2022: a hub for mass spectrometry-based proteomics evidences. *Nucleic Acids Res* **50**, D543–D552 (2021).

110. Yu, N. Y. *et al.* PSORTb 3.0: improved protein subcellular localization prediction with refined localization subcategories and predictive capabilities for all prokaryotes. *Bioinformatics* **26**, 1608–1615 (2010).

Acknowledgments

We thank Dr. Alice Lebreton, Dr. Julie Guignot, Dr. Benoit Garin, Dr. Lauriane Quenee, Dr. Clément Carré, Pr. Gunter Meister, Dr. Hervé Le Hir for providing the *Staphylococcus aureus* SH1000 genomic DNA, *Pseudomonas aeruginosa* PAO1 strain and *Escherichia coli* O157:H7 gDNA, *Bordetella pertussis* Tohama gDNA, *Yersinia pestis* gDNA, AutomiG reporter, a vector expressing T6B, pET22-$_6$His-SUMO and pET28-CBP-$_6$His, respectively. We thank Dr. Sophie Goudey for the generation of KO HeLa cell lines. We also thank all members of the Navarro lab for their inputs, discussions and critical reading of the manuscript, as well as Dr. Alice Lebreton, Dr. Michael Mourez, and Miss Isabelle Barbosa for helpful advices and discussions. This work was supported by the European Research council (281749, Silencing & Immunity, to L.N.), a grant from the European Molecular Biology Organization (EMBO) Young Investigator Program (to L.N.), an Action Thématique et Incitative sur Programme (ATIP)/Avenir Grant from the Fondation Bettencourt Schueller (FBS, to

L.N.), an Emergence Grant from the Mairie de Paris (to L.N.), a CIFRE PhD program from the Association Nationale Recherche Technologie (ANRT, 2017/0009 to J.T), a fourth-year PhD programme from the Fondation pour la Recherche Médicale (FRM, FDT202001010790 to J.T.) and a grant ANRS (ECTZ47170 to S.G.M.). Work in the C.B. laboratory was supported by the Institut Pasteur, the FRM grant N° EQU201903007847 and the Agence Nationale de la Recherche grant n°ANR-10-LABX-62-IBEID.

Author contributions

Conceptualization, J.T. and L.N.; Software J.T., L.S. and D.F.; Validation, J.T. and L.N.; Formal analysis, J.T. and B.L.; Investigation, J.T., M.R., M.C., D.F., L.S., K.A.S., H.C.V, C.R., B.L. and L.N.; Resources, S.G-M and A.A; Data curation B.L. and D.L.; Writing – original draft, J.T. and L.N.; Review & Editing, J.T., C.B., L.N.; Visualization, J.T. and L.N.; Supervision, C.B., A.A., D.L. and L.N.; Project Administration, J.T. and L.N.; Funding acquisition, J.T., C.B. and L.N.

Competiting interests

M.R, M.C., D.F., L.S., K.A.S, H.C.V, S.G-M., B. L., D.L., C.B. and L.N declare no competing interests. J.T. is a recipient of an EVOTEC funded PhD fellowship in the context of the French private-public partnership CIFRE program from the ANRT. A.A. is an EVOTEC employee.

Figure legends

Figure 1. LegK1 suppresses siRNA- and miRNA- guided gene silencing through both its kinase activity and its predicted Ago-binding platform

a Schematic representation of the LegK1 protein sequence. The position and amino acid sequence of three selected W-motifs (W41, W283, W293 motifs) recovered from the Wsearch analysis are depicted. The lysine 121 is located inside the ATP-binding pocket of the serine/threonine kinase of LegK1 and is required for catalytic activity. TD, transmembrane domain. **b** The LegK1-KA and LegK1-3WF mutant proteins are stable in human cells. HEK293T cells were transfected with vectors expressing either Flag-eGFP, 2xFlag-LegK1 (WT), 2xFlag-LegK1-KA or 2xFlag-LegK1-3WF proteins for 48 hours. Immunoblot was performed using an anti-Flag antibody. **c** A *GFP*-based siRNA reporter is silenced by both Ago1 and Ago2. *GFP*-based silencing reporter assay in control (CTL), *ago1*$^{-/-}$, *ago2*$^{-/-}$, *ago1/2*$^{-/-}$, and *dicer*$^{-/-}$ HeLa cell lines. HeLa cell lines were co-transfected with vectors expressing *eGFP* and control siRNAs (siCTL) or *GFP* siRNA duplexes (siGFP). At 48h post-transfection, cell lysates were subjected to Western Blot analysis with indicated antibodies. The eGFP protein levels are relative to the ones of GAPDH and further normalized to the corresponding siCTL condition, as indicating above the GFP blot. **d** YopM does not alter the silencing of the GFP-based siRNA reporter. *GFP*-based silencing reporter assay in the presence of empty vector (Vec) or YopM in HEK293T cells. The experiment and the eGFP protein quantification were performed as described in (**c**). **e** LegK1 suppresses silencing of a *GFP*-based siRNA reporter through both its kinase activity and W-motifs. *GFP*-based silencing reporter assay in the presence of LegK1 WT, LegK1-KA or LegK1-3WF in HEK293T cells. The experiment was performed as described in (**c**), but the vector

expressing Flag-YopM, 2xFlag-LegK1-KA, 2xFlag-LegK1-3WF or Flag-T6B were co-transfected along with the reporter system. The eGFP protein levels were quantified as described in (**c**). **f** YopM does not alter the silencing of a *GFP*-based miRNA reporter. HEK293T cells were co-transfected with the AutomiG vector and the empty vector (Vec) or vector expressing Flag-YopM for 48 hours. The GFP protein levels are relative to the ones of GAPDH and further normalized to the empty vector condition, as depicting at the top of the GFP immunoblot. **g** LegK1 suppresses silencing of the *GFP*-based miRNA reporter through both its kinase activity and W-motifs. AutomiG silencing reporter assay in the presence of LegK1 WT, LegK1-KA or LegK1-3WF was conducted in HEK293T cells. The experiment, and the GFP quantification, were performed as described in (**f**), but normalised to the YopM control condition.

All data are representative of three independent experiments. GAPDH was used as a loading control in all these experiments. * represents aspecific bands.

Figure 2. LegK1 interacts with components of the miRISC and directly binds to Ago2 and its PIWI domain

a and **b** LegK1 interacts with Ago proteins and components of the miRISC through its W-motifs. HEK293T cells were transfected with vector expressing Flag-eGFP, 2xFlag-LegK1 WT, 2xFlag-LegK1-KA or 2xFlag-LegK1-3WF. At 48h post-transfection, cells were lysed and proteins were immunoprecipitated using an anti-Flag antibody. Total cell lysates (input) and the immunoprecipitates were analyzed by immunoblotting using indicated antibodies. **c** LegK1 interacts with Ago2 in a RNA-independent manner. HEK293T cells were transfected with a vector expressing 2xFlag-LegK1 or co-transfected with vectors expressing 2xFlag-LegK1 and GFP-Ago2. At 48h post-transfection, cells were lysed, incubated with or without RNase A, and proteins were

further immunoprecipitated using an anti-Flag antibody. Total cell lysates (input) and the immunoprecipitates were analyzed by immunoblotting using indicated antibodies. **d** Schematic representations of the recombinant proteins used for *in vitro* pull-down assays. CBP, Calmodulin Binding Protein; GST, Glutathione S-Transferase; SUMO, Small Ubiquitin-like MOdifier; TD, Transmembrane Domain. **e** LegK1 directly interacts with Ago2 *in vitro*. Pull-down assay between human Ago2 and LegK1 recombinant proteins. GST-Ago2 was incubated with His_6-SUMO-LegK1 (a.a. 2:386) or His_6-TAP used as negative control, and subjected to a GST pull-down assay. **f** LegK1 directly interacts with the PIWI domain of Ago2 *in vitro.* Pull-down assay between the PIWI domain of human Ago2 and LegK1 recombinant proteins in the absence or presence of RNAs. CBP-PIWI-His_6 (a.a. 517-817) or His_6-TAP, which consists in a CBP tag used as negative control, were incubated with His_6-SUMO-LegK1 (a.a. 2:386), with or without RNAs extracted from human cells, and subjected to a CBP pull-down assay. All data are representative of three independent experiments. GAPDH was used as a loading control. * represents an aspecific band.

Figure 3. The W283 and W293 motifs of LegK1 bind to human Ago proteins and exhibit sequence conservation among the homologs of *Legionella*

a Schematic representation of LegK1 from *L. pneumophila* along with the synthetic biotinylated peptides used for pull-down assays. Each peptide sequence containing the WT (W1, W2, W3) or mutated versions (F1, F2, F3, A3) of predicted W-motifs of LegK1 are depicted. **b** and **c** Immunoprecipitations of W-motif-containing peptides from HEK293T cells. Synthetic biotinylated peptides were mobilized on streptavidin beads, incubated with HEK293T cell lysates and further immunoprecipitated. Incubation of beads without peptides was used as negative control (no pept.). The

presence of the human Ago proteins in cell lysate (input) and bound to the beads was assessed by immunoblotting using the indicated antibodies. **d** Alignment of LegK1 homologs from *Legionella* species around the three putative W-motifs. The protein sequence of LegK1 (*lpp1439* gene) from *Legionella pneumophila* strain Paris was used as a reference sequence to determine the presence of homologs in *Legionellales* order (taxid: 445). An identity cutoff of 40%, an Expect (*E*)-value cutoff of 10^{-5} and a minimum percentage match length of subject and query of 65% were used. The set of homologous protein sequences was aligned using ClustalW2. **e** Schematic representation of LegK1 homologs from *L. quateirensis* along with the synthetic biotinylated peptide used for pull-down assays. **f** Immunoprecipitations of the peptides corresponding to the homologous W283-motif of *L. quatereinsis* from HEK293T cells, as depicted in (**b**) and (**c**).

All data are representative of three independent experiments. GAPDH was used as negative control.

Figure 4. The kinase, RNA silencing suppression and NF-κB signaling activation activities of LegK1 are interconnected

a The LegK1-W293A and LegK1-W283F-W293A mutants are altered in their ability to phosphorylate IκBα. Kinase assay in the presence of LegK1 mutants. HEK293T cells were transfected with vectors expressing Flag-eGFP, 2xFlag-LegK1 WT, 2xFlag-LegK1-W283F, 2xFlag-LegK1-W293F, 2xFlag-LegK1-W293A and 2xFlag-LegK1-W283F-W293A. At 48h post-transfection, cells were lysed and subjected to a Flag immunoprecipitation. The resulting immunoprecipitates were incubated with purified CBP-IκBα-His_6 recombinant proteins. The phosphorylation of the serine 32 of IκBα was analyzed by immunoblotting using a specific antibody. * represents aspecific

bands. **b** The LegK1-W293A and -W283F-W293A mutants are altered in their ability to suppress silencing of the *GFP*-based siRNA reporter. *GFP*-based siRNA silencing reporter assay was performed in the presence of LegK1 mutant versions in HEK293T cells. Cells were co-transfected with pFlag-eGFP, negative control siRNA (siCTL) or GFP RNA duplexes, and vector expressing Flag-YopM, 2xFlag-LegK1 WT, 2xFlag-LegK1-W283F, 2xFlag-LegK1-W293F, 2xFlag-LegK1-W293A or 2xFlag-LegK1-W283F-W293A for 48 hours. The eGFP protein levels are relative to the ones of GAPDH and further normalized to the YopM control condition (with siCTL), as depicting at the top of the GFP immunoblot. **c** The silencing suppression of the *GFP*-based siRNA reporter triggered by LegK1 is in part dependent on its ability to activate NF-κB signaling. *GFP*-based siRNA silencing reporter assay was performed in the presence of LegK1 in HEK293T cell line treated with CAPE. The experiment was performed as described in (**b**). Cells were treated with DMSO or 25 μg/mL of CAPE for 1h. The phosphorylation of the serine 32 of IκBα was used as a marker of NF-κB signaling activation. The eGFP protein levels are relative to the ones of GAPDH and further normalized to the empty vector (Vec) control condition (with siCTL), as indicating at the top of the GFP immunoblot.

The results shown are representative of two (**a**) or three (**b**) and (**c**) independent experiments. GAPDH was used as a loading control.

Figure 5. LegK1 is a key virulence factor from *L. pneumophila* that promotes bacterial growth in human macrophages by genetically targeting Ago4

a LegK1 promotes *L. pneumophila* growth in *A. castellanii*. *A. castellanii* were infected with *Lpp* WT and Δ*legK1* mutant strains at a MOI of 0.1. Intracellular replication was determined by recording the number of colony-forming units (CFU) by plating on

buffered charcoal yeast extract (BCYE) agar. Results are shown as log10 ratio CFU/mL, where CFUs were normalized with the associated condition at 1h post-infection, corresponding to the entry of bacteria in host cells. **b** LegK1 promotes *L. pneumophila* growth in human macrophages. THP-1 monocyte-derived macrophages were infected with *Lpp* WT or Δ*legK1* mutant strain at a MOI of 10. Results are shown as log10 ratio CFU/mL, where CFU were normalized with the associated condition at 2h post-infection, corresponding to the entry of bacteria in host cells. **c** Complementation assays in *A. castellanii.* Cells were infected at a MOI of 1 with *Lpp* WT or Δ*legK1* mutant strains carrying the empty vector pBC-KS (Vec) or *Lpp* Δ*legK1* mutant carrying the complementing plasmid pBC-KS-LegK1. Intracellular growth was determined as in (**a**). **d** Complementation assays in THP-1 cells. Cells were infected at a MOI of 10 with the *Lpp* WT and Δ*legK1* mutant carrying the empty vector pBC-KS (Vec), or *Lpp* Δ*legK1* mutant carrying the pBC-KS-legK1 complementing plasmid. Intracellular growth was determined as in (**b**). **e** Heatmap of the four Ago transcript levels in HEK-TE, A549 and THP-1 cell lines. The RNA-sequencing data were recovered from the Cancer Cell Line Encyclopedia (Primary ID: E-MTAB-2770) and are reported as linear values. **f** Immunoblot of Ago2 and Ago4 in HEK293T, A549 and THP-1 cell lines. **g** Immunoblot of Ago2 and Ago4 in *ago2*$^{-/-}$ and *ago4*$^{-/-}$ CRISPR-Cas9-based knockout THP-1 cell lines. GAPDH was used as a loading control. **h** The growth defect of the *Lpp* Δ*legK1* strain is rescued in human macrophages depleted of Ago4. Intracellular replication of the *Lpp* WT or Δ*legK1* mutant strain was determined in THP-1 monocytes-derived macrophages depleted of Ago2 or Ago4. WT, *ago2* $^{-/-}$ and *ago4* $^{-/-}$ THP-1 macrophages were infected with *Lpp* WT or Δ*legK1* strains at a MOI of 10. Bacterial titers were monitored at 24 hours post-infection (*hpi*) and were analysed as described in (**b**).

Data are represented as ± SD. Data are representative of three (A, C, F and G) or seven (**b**) and (**h**) independent experiments. Plotted data of THP-1 WT infections in (**c**) are the same as the data shown in (**h**) at 24 *hpi*. *, $P < 0.05$; NS, not significant, as calculated using Wilcoxon test.

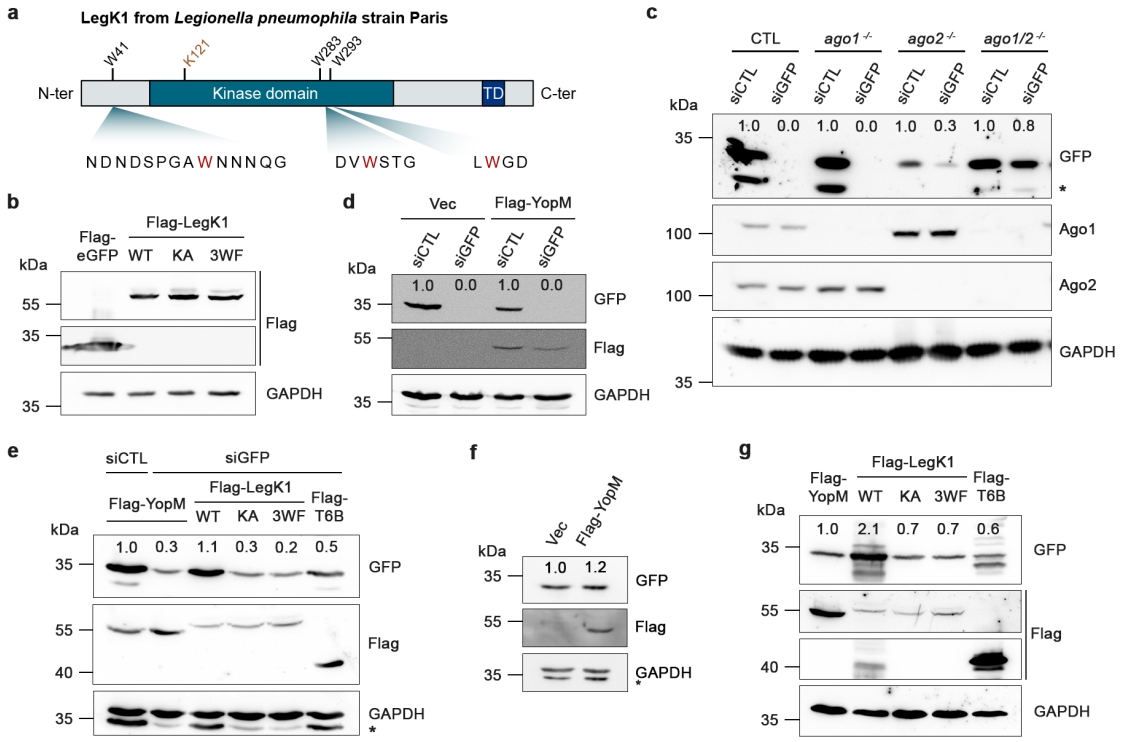

Figure 1. LegK1 suppresses siRNA- and miRNA- guided gene silencing through both its kinase activity and its predicted Ago-binding platform

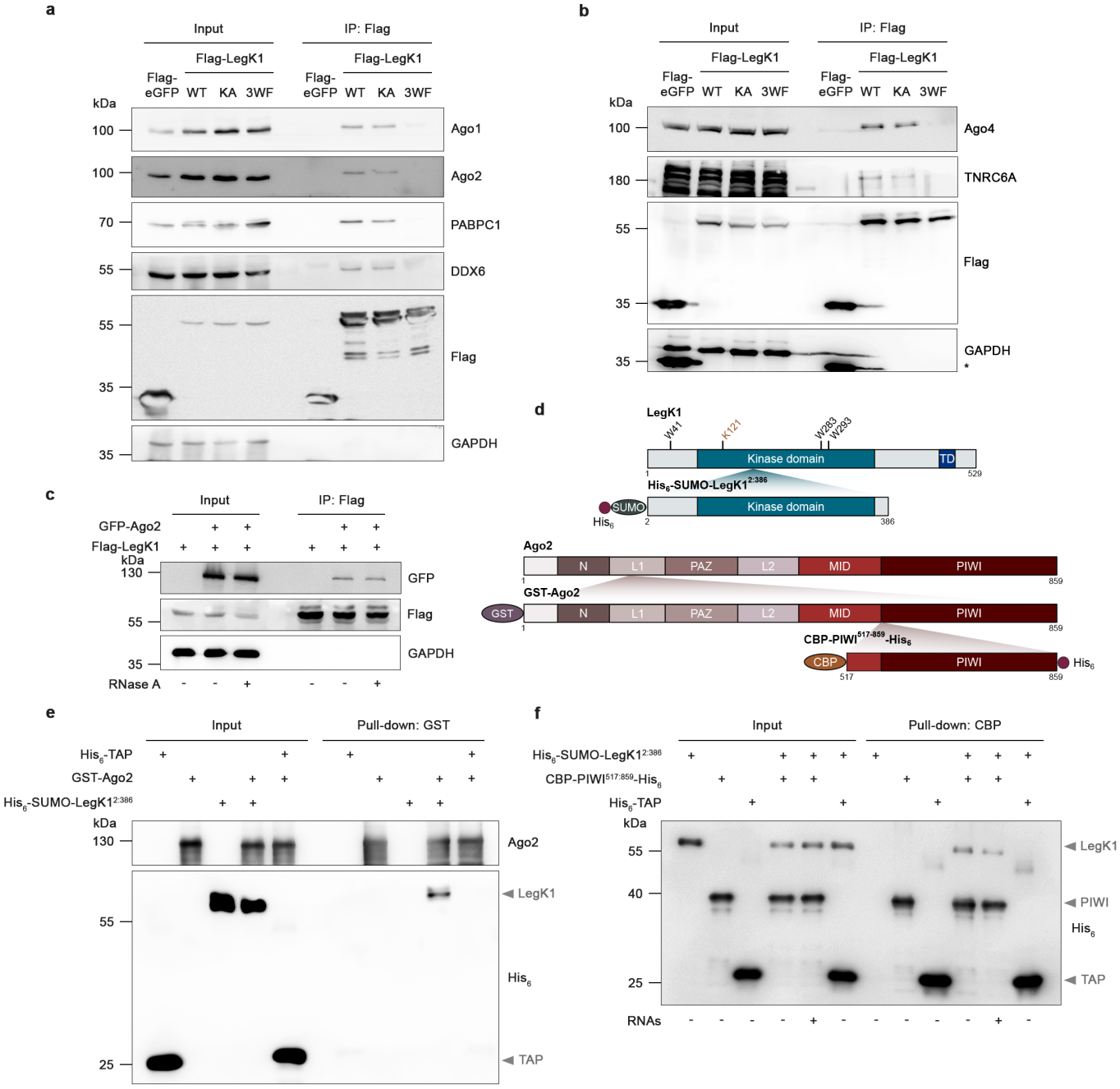

Figure 2. LegK1 interacts with components of the miRISC and directly binds to Ago2 and its PIWI domain

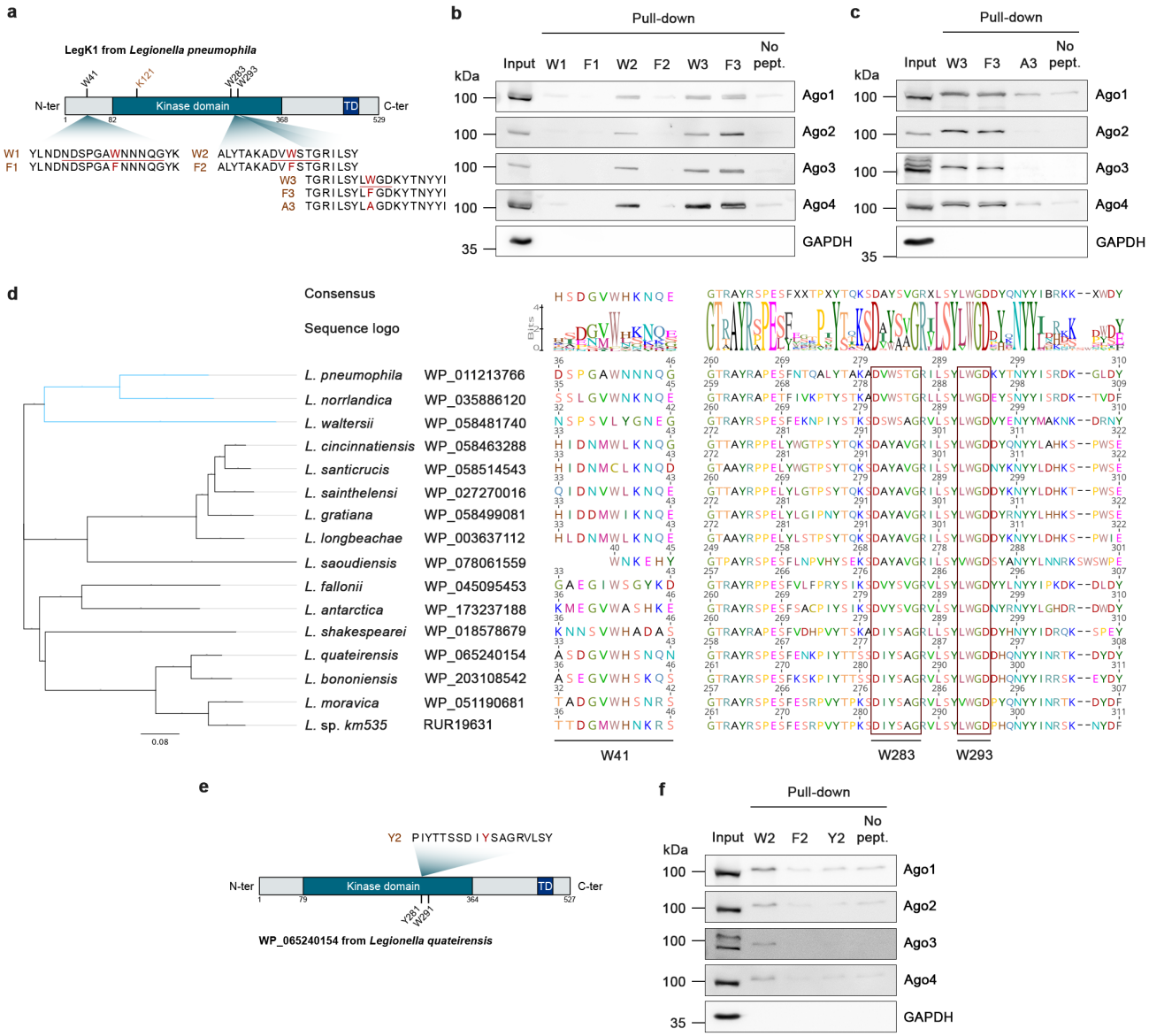

Figure 3. The W283 and W293 motifs of LegK1 bind to human Ago proteins and exhibit sequence conservation among the homologs of *Legionella*

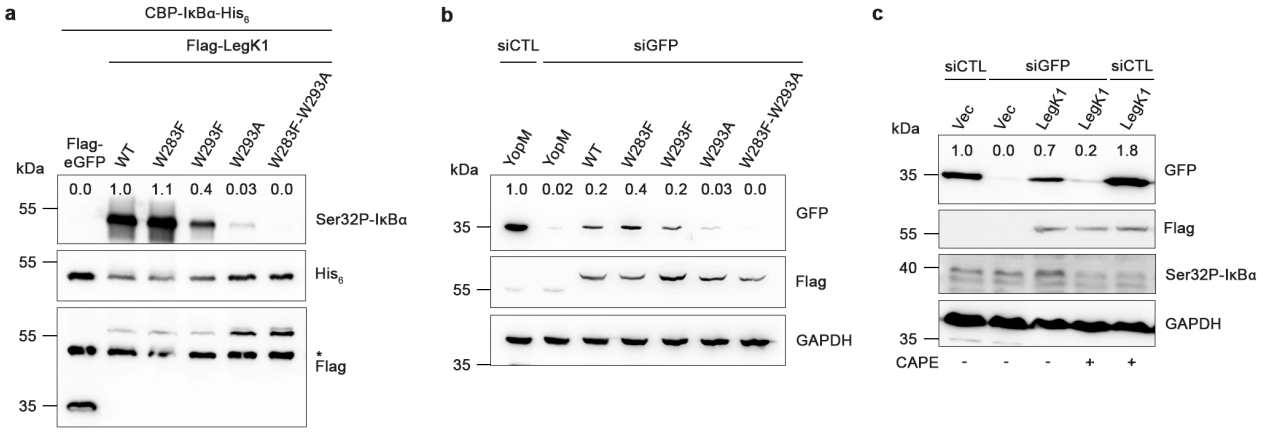

Figure 4. The kinase, RNA silencing suppression and NF-kB signaling activation activities of LegK1 are interconnected

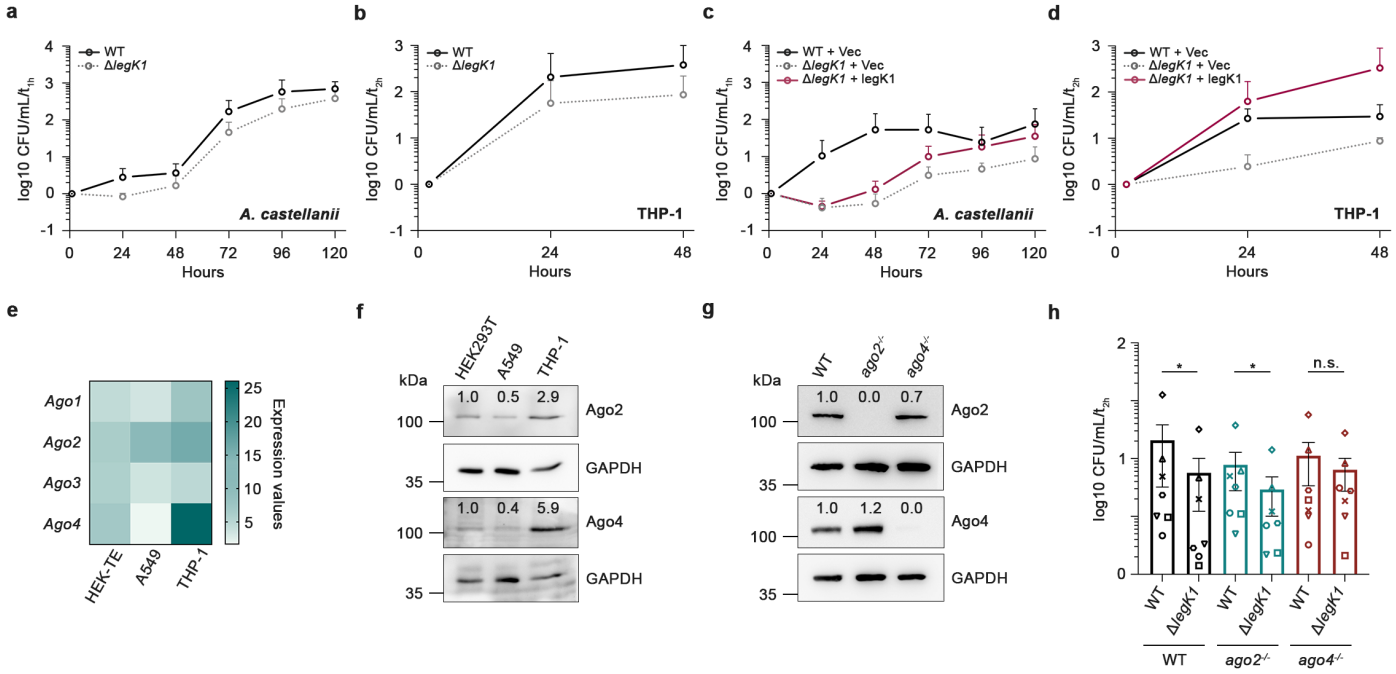

Figure 5. LegK1 is a key virulence factor from *L. pneumophila* that promotes bacterial growth in human macrophages by genetically targeting Ago4